United States
Department of
Agriculture

Forest Service

Forest
Products
Laboratory

U.S. DOT
Federal Highway
Administration

Research
Paper
FPL–RP–553

Experimental Shear Strength of Unchecked Solid-Sawn Douglas-fir

Douglas R. Rammer
Lawrence A. Soltis
Patricia K. Lebow

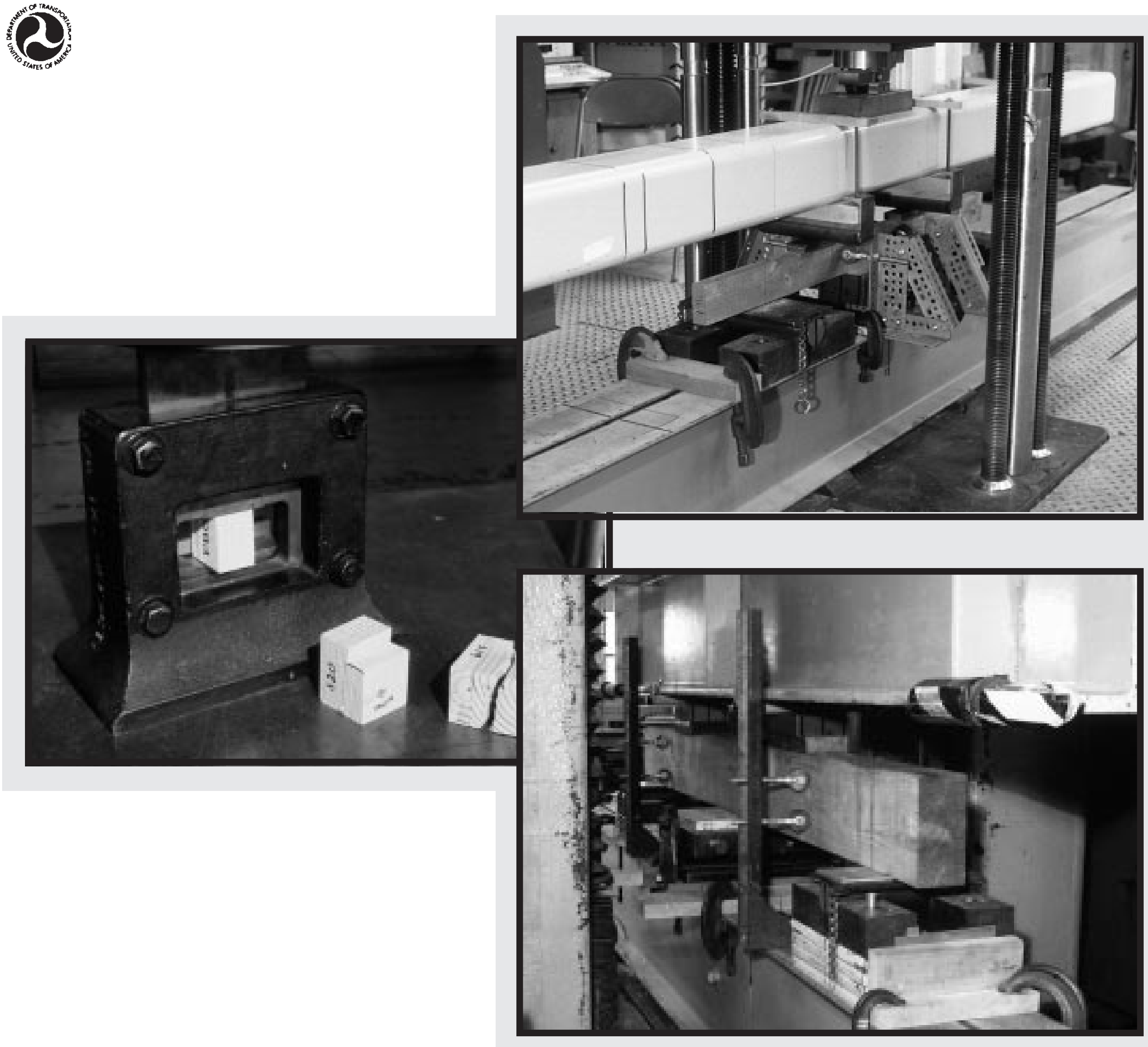

Abstract

This report presents experimental results of modulus of rupture and shear strength tests on unsplit, green, sawn Douglas-fir lumber. Five different size-matched specimens, ranging from nominal 2- by 4-in. (standard 38- by 89-mm) to nominal 4- by 14-in. (standard 95- by 343-mm), were tested in third-point bending and five-point beam shear. A total of 120 bending and 160 shear specimens, as well as shear blocks cut from each beam, were tested. Results adjusted to 12 percent moisture content are compared with results from prior research on Douglas-fir glued-laminated timber beams. Statistical methods were used to investigate possible correlations of shear strength to beam size, shear strength to bending strength, and beam shear strength to ASTM shear block strength. The results indicate that (1) a five-point test setup can consistently produce beam shear failures over a wide range of beam sizes, (2) shear strength is dependent on beam shear area, (3) beam shear strength is related to ASTM D143 shear block strength values provided that the re-entrant corner stress-concentration effects are considered, and (4) a low correlation exists between modulus of rupture and shear strength.

Keywords: Beam, design, shear strength, shear stress, modulus of rupture, shear test, modulus of elasticity

September 1996

Rammer, Douglas R.; Soltis, Lawrence A.; Lebow, Patricia K. 1996. Experimental shear strength of unchecked solid-sawn Douglas-fir. Res. Pap. FPL–RP–553. Madison, WI: U.S. Department of Agriculture, Forest Service, Forest Products Laboratory. 33 p.

A limited number of free copies of this publication are available to the public from the Forest Products Laboratory, One Gifford Pinchot Drive, Madison, WI 53705–2398. Laboratory publications are sent to more than 1,000 libraries in the United States and elsewhere.

The Forest Products Laboratory is maintained in cooperation with the University of Wisconsin.

Acknowledgments

We express sincere appreciation to the following agencies and individuals who contributed to the success of this project: the Federal Highway Administration, for joint funding with the Forest Products Laboratory under cooperative research agreement FP-94-2266; Michael Ritter of the Forest Products Laboratory, for support and interest in the research; and Kathy Scarince and Javier E. Font of the Forest Products Laboratory, for assistance in various laboratory experiments.

Contents

Page

Introduction 1
Background 2
Research Methods 4
  Materials 4
  Beam Shear Tests 4
  Bending Tests 4
  Failure Definition 6
  Measurements 6
  Shear Block Tests 7
Analysis 7
  Maximum Stress Calculations 7
  Elastic Modulus Calculations 8
  Moisture Adjustments 8
  Specific Gravity Adjustments 9
  Censored Statistics Calculations 9
Results 10
  Shear Tests 10
  Bending Tests 10
  Shear Block Tests 10
Discussion 13
  Dry/Green Ratio and Specific Gravity–Shear Strength Relationship 14
  Shear Strength to Beam Size Relationship 15
  Shear Block to Beam Shear Relationship 18
  Comparison of Solid-Sawn and Glued-Laminated Beam Shear 19
  Shear to Bending Strength Relationship 20
Conclusions 20
Literature Cited 21
Appendix A—Details of Experimental Deflection Procedures 23
Appendix B—Five-Point Shear Results for Solid-Sawn Douglas-fir 24
Appendix C—Third-Point Bending Results for Solid-Sawn Douglas-fir 29

Experimental Shear Strength of Unchecked Solid-Sawn Douglas-fir

Douglas R. Rammer, Engineer
Lawrence A. Soltis, Supervisory Research Engineer
Patricia K. Lebow, Mathematical Statistician
Forest Products Laboratory, Madison, Wisconsin

Introduction

Mechanical properties of lumber were historically determined from small, straight-grained, clear specimens. The clear wood values established a baseline from which allowable design values were derived according to American Society for Testing and Materials (ASTM) procedures. In recent years, allowable mechanical values have been based on full-sized structural members. In a cooperative effort, the United States and Canada conducted the In-Grade program to establish some mechanical properties of most commercial softwood species and grades of lumber in both countries. Standardized methods for testing the modulus of elasticity, modulus of rupture, compression strength parallel-to-grain, and tension strength parallel-to-grain properties in ASTM D1990 (ASTM 1995) were established for this effort. At the time of the In-Grade program, no standardized method was available for testing structural members for shear strength. Therefore, current allowable shear strength values are still based on a small, clear specimen procedure set forth in ASTM D245 (ASTM 1995).

Ethington and others (1979) traced the evolution of allowable shear stress values since about 1900 to explain the development of the ASTM D245 factors. Currently, ASTM D245 adjusts the 5-percent percentile shear-strength values of ASTM D2555 (ASTM 1995) for clear, straight-grained softwood species by an adjustment factor of 1/4.1 and a strength ratio of 1 to 0.50. The adjustment factor consists of three subfactors:

1. stress concentration of 0.44, which accounts for the stress riser at the end of checks
2. duration of load of 0.62, which adjusts 10-min test data to accumulated 10-year live-load expectancy
3. experience factor of 0.89

The strength ratio adjusts for splits, checks, or shakes. A 0.5 adjustment is taken when the defect is equal in length to the wide face measurement.

The ASTM D245 adjustment factors are a direct result of the inability to create a high percentage of shear failures in wood beams and Newlin's early influence on design stress values. The shear strength of ASTM D143 (ASTM 1995) shear blocks is higher than the shear strength observed from tests of beams. Therefore, to determine a realistic relationship between the shear strength of clear wood and beams, a new test method was developed for beam shear strength that is applicable to a range of beam sizes.

Rammer and Soltis (1994) experimentally tested the shear strength of Southern Pine and Douglas-fir glued-laminated beams with a five-point beam shear setup. This work indicated that shear strength varies with beam size and may be correlated to the standard ASTM D143 shear block values. The research reported here is an extension of this work to solid-sawn Douglas-fir. The objective of this study was to improve current shear design criteria by

- establishing a data base for beam shear strength of solid-sawn Douglas-fir lumber and correlating it to shear block test results,
- verifying if the beam-size equation for shear strength and beam size is valid for solid-sawn material,
- determining whether shear strength is more dependent on shear area, volume, or depth for modeling purposes, and
- determining if there is a correlation between shear and bending strength.

Background

In the early 1900s, small clear test specimens were recognized as having higher shear strength than larger beam members (Ethington and others 1979). In the mid 1920s, the ASTM adopted a standard shear block test method for clear wood proposed by the USDA Forest Service, Forest Products Laboratory. The ASTM D143 (ASTM 1995) shear block test consists of a 2- by 2- by 2.5-in. (51- by 51- by 64-mm) clear wood specimen with a 2- by 2-in. (51- by 51-mm) failure surface (Fig. 1). Results of this test, in conjunction with techniques outlined in ASTM D2555 (ASTM 1995), determine shear strength values for green, clear, straight-grained wood. The ASTM D245 procedure (ASTM 1995) modifies these shear strength values to derive allowable design values for lumber. One criticism of this procedure lies in the strength values of the ASTM shear block.

The ASTM shear block test does not result in pure shear failures since moments and local stress concentrations are present across the failure plane. The stress concentration at the re-entrant corner of the shear block has raised a question of the adequacy of the test for determining realistic shear strength values. Rammer and Soltis (1994) reviewed the effect of the re-entrant corner on the shear stress distribution in the ASTM shear block test. By summarizing both experimental and finite element studies, the authors showed that the ASTM assumed shear strength (τ_{ASTM}) is less than the true failure stress (τ_{fail}) by a factor of about 2.0.

The results from ASTM D143 clear wood shear block specimens are not representative of the shear strength of structural beams and do not account for local defects: checks, splits, and knots. Attempts to characterize the decreased shear strength with increased beam size began in the 1960s. Huggins and others (1966) observed shear strength variation during a Canadian bridge stringer research project. They concluded that shear strength is a function of beam depth and shear span, where shear span is defined as the distance between a support and the nearest concentrated load. They stated that shear strength generally tends to decrease as the shear span-to-depth ratio increases. They also observed that shear strength decreases to an asymptotic level for large span-to-depth ratios.

Keenan (1974) reviewed prior research studies in which shear failures had occurred and found a relationship between shear strength and beam size. He also conducted tests on small clear specimens and used finite element models to indicate that the shear strength of Douglas-fir glued-laminated beams depended on the sheared area. Keenan defined sheared area as the shear span, as defined by Huggins and others (1966), multiplied by beam width. This parameter is easily defined for members loaded by concentrated loads, but is undefined for uniformly distributed loads.

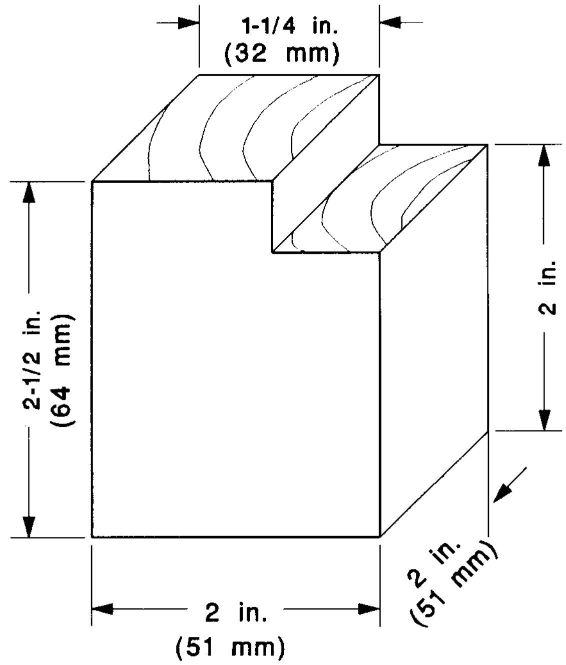

Figure 1—ASTM shear block.

Keenan also concluded that the two-beam theory proposed by Newlin and others (1934) is not applicable to glued-laminated beams.

Foschi and Barrett applied the Weibull theory (Weibull 1939) to the tension and shear strength of wood. Barrett (1974) applied the theory to the tension perpendicular to grain, and Foschi and Barrett (1976,1977) applied the theory to the shear strength of wood. These authors related shear strength to an integrated stress volume defined by Weibull theory.

The Weibull theory is a statistically based theory for predicting the strength of a material. The theory is most applicable to predicting the strength of brittle materials. The following equation is the basis for the theory:

$$P = 1 - e^{\int \eta(\sigma)dV} \tag{1}$$

This equation is based on the premise that a larger volume will contain more strength-reducing flaws than a smaller volume. Probability of fracture, P, is related to $\eta(\sigma)$, a positive nondecreasing function, and volume V. Weibull proposed a two parameter relationship of

$$\eta(\sigma) = \left(\frac{\sigma}{\sigma_0}\right)^m \tag{2}$$

which is related to observed experimental results. The m parameter characterizes the flaws in a material, and the σ_0

parameter is a reference stress level. After applying the theory to a wider array of experimental results, Weibull added a parameter σ_u to account for the truncation of data by specimen formation process by setting a level of stress below which the component will never fail. The three parameters are determined from experimental data.

The stress parameter σ is a function of beam depth, span, and width; therefore, the stress distribution from loading and material parameters together define the risk of fracture of a given material. Using Weibull theory for shear strength prediction is difficult since the stress distribution requires numerical integration of the volume integral. Foschi and Barrett performed these calculations for various loadings and proposed a design procedure to account for shear stress variation. This approach has been adopted in Canadian standards (CSA 1984).

Longworth (1977) experimentally verified that the ASTM shear block strength is not representative of beam strength and that beam size, sheared area, or volume appreciably affects shear strength. He tested 150 glued-laminated Douglas-fir beams, manufactured following the Canadian CSA 0177 qualifications, using a four-point bending test with small length-to-depth (l/d) ratios. Plots of shear strength as a function of Keenan's shear area show higher strength values for small shear areas and asymptotically decreasing values for larger shear areas.

Quaile and Keenan (1978) created a specially designed glued-laminated material beam shear test to maximize shear failure in rectangular beams. This test specimen configuration successfully produced shear failures in 104 of 108 specimens tested, and gave further evidence that the ASTM shear block test produces lower strength values than is evident in small rectangular beams. Using the special test specimen, Keenan and others (1985) determined the shear strength of spruce glued-laminated beams. The study focused on a range of factors—from small clear specimens to standard glued-laminated sizes and three species of spruce (white, black, and eastern). The authors concluded that shear strength is a function of sheared area, not volume.

Rammer and Soltis (1994) tested both Southern Pine and Douglas-fir glued-laminated beams in five-point bending. The results showed a high percentage of beam shear failures: 102 of 138 Southern Pine and 170 of 192 Douglas-fir beams failed in shear. The authors concluded that shear strength is a function of shear area and is related to the ASTM shear block through the following equation:

$$\tau = \frac{1.3 C_f \tau_{ASTM}}{A^{1/5}} \qquad (3)$$

where

τ is beam shear strength (lb/in^2),
C_f stress concentration factor to adjust the ASTM shear block assumed value to true maximum stress,
τ_{ASTM} ASTM D143 published shear block value, and
A shear area (area of beam subjected to shear forces).

Rammer and Soltis's definition of shear area differs from that of Keenan and others (1985), who defined shear area as shear span times beam width, where shear span was defined as the length of the beam under positive shear. In the work reported here, shear area is defined as the length under both positive and negative shear in the region of high shear. This definition results in a shear area equivalent to twice Keenan's defined area for most cases encountered in engineering design.

Additional collaboration of the shear strength–beam size equation developed by Rammer and Soltis (1994) is observed using data generated by the American Plywood Association (APA) (Yeh 1993). The APA conducted simply supported shear tests on 115 Douglas-fir glued-laminated beams. Their data exhibited similar strength values and fell within the variability of Longworth's and Rammer and Soltis's studies on Douglas-fir glued-laminated beams, as shown in Figure 2.

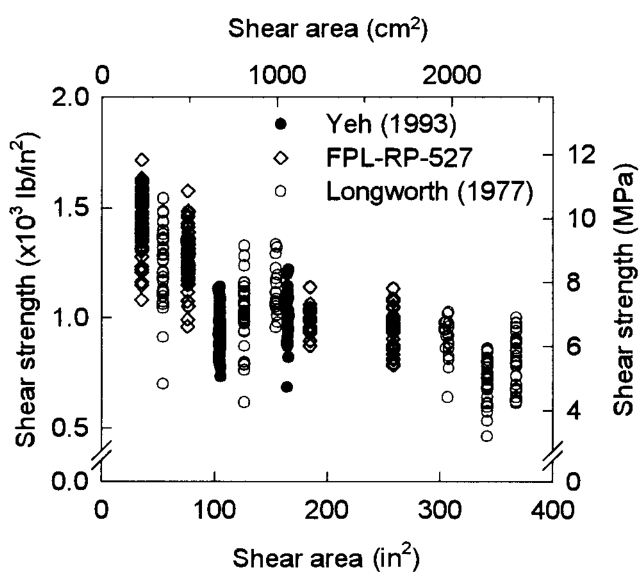

Figure 2—Comparison of various data for relationship of shear strength to shear area for Douglas-fir glued-laminated beams. APA T93-2, Yeh (1993); FPL 527, Rammer and Soltis (1994); Longworth (1977).

Research Methods

Shear and bending strengths of specimens matched by stress-wave elastic modulus values were determined for green Douglas-fir beams of several sizes. Five-point bending specimens were tested to determine beam shear strength. Third-point bending specimens were tested to determine modulus of rupture and modulus of elasticity. Solid-sawn beam strength and shear block strength were related through ASTM D143 shear blocks cut from each test specimen.

Materials

A total of 680 green No. 2 grade or better Douglas-fir (*Pseudotsuga menziesii*) beams were obtained from a lumber mill located near Portland, Oregon, for determination of shear and bending strength properties. Nominal dimensions ranged from 4 in. by 14 in. by 18 ft (standard 89 mm by 343 mm by 5.49 m) to 2 in. by 4 in. by 10 ft (standard 38 mm by 89 mm by 3.05 m). The number and average size of each member group are listed in Table 1. (Beams will hereafter be referred to by their nominal dimensions: 2 by 4, 2 by 10, etc.) Upon arrival at the Forest Products Laboratory, each size of shear specimens was sorted into three groups and each size of bending specimens was sorted into two groups based on stress-wave elastic modulus values. Thus, the statistical distribution of modulus of elasticity was matched between bending and shear specimen groups for each size except the 2 by 4 beams. For this size, both bending and shear specimens were cut from one 10-ft- (3-m-) long stock member, resulting in end-matched specimens. One group from each size was tested in this study. The remaining material will be used for future studies on shear strength. A flowchart of the complete testing program is shown in Figure 3.

All material was stacked in an uncontrolled environment until testing. Periodic moisture readings were taken to ensure that specimen moisture content did not drop below 20 percent. Specimens were watered periodically to maintain a moisture content greater than 20 percent. Testing was conducted during the fall and winter months. To ensure that temperature did not affect the results of strength tests, specimens were moved inside at least 24 h before testing. Preliminary tests using thermocouples determined that this was an appropriate length of time to thoroughly warm the specimens.

Beam Shear Tests

A five-point bending test setup was used to maximize the number of shear failures. This setup was previously used to determine the shear strength of Southern Pine and Douglas-fir glued-laminated beams (Rammer and Soltis 1994). The setup consisted of a two-span beam with concentrated loads symmetrically placed on either side of the center support, resulting in larger shear forces than could be obtained by a single-span test setup. Each setup had an overall length of 10*d*, where *d* is the actual depth of the specimen, and individual center-to-center spans of 5*d*. Figure 4 shows the general setup, and Table 2 lists dimensions for the test setups.

Table 1—Dimensions and number of solid-sawn Douglas Fir test specimens

Test	Nominal dimensions	Actual average beam size: Width in.	(mm)	Depth in.	(mm)	Number of specimens
Shear	2 by 4	1.44	(37)	3.43	(87)	40
	2 by 10	1.42	(36)	9.32	(237)	40
	4 by 8	3.89	(99)	7.97	(202)	40
	4 by 12	3.85	(98)	11.88	(302)	20
	4 by 14	3.76	(95)	13.78	(350)	20
Bending	2 by 4	1.46	(37)	3.45	(88)	40
	2 by 10	1.46	(37)	9.35	(238)	20
	4 by 8	3.87	(98)	7.95	(202)	20
	4 by 12	3.81	(97)	11.74	(298)	20
	4 by 14	3.80	(97)	13.79	(350)	20

Special attention was given to the load application points. Large loads needed to produce shear failures also created excessive compression perpendicular-to-grain deformation under the loading points. To limit these effects, the load and support plates were designed to limit the compression perpendicular-to-grain stress to below 1,000 lb/in^2 (6.89 MPa) at failure. Since shear strength of the beam increases with smaller sizes, proportionally higher compression stresses are developed for smaller beams. Thus, as the beam size decreased, the relative distance between the end of the middle plate and the end of the loading plate was decreased.

Bending Tests

Third-point bending tests on simple spans were conducted to determine the modulus of rupture and bending modulus of elasticity of the Douglas-fir beams. All beams tested had a span of 15*d*, except the 4 by 8 specimens. These specimens were tested on a 14*d* span because they were not long enough to test on a 15*d* span and have full end bearing. Loads were placed symmetrically around the centerline at a distance of 2.5*d*. Small, flat sliding plates distributed the load so that compression perpendicular to grain did not influence the strength results. Figure 5 shows the general setup, and Table 3 lists setup dimensions for the tests. This setup conforms to ASTM D198 §8.5.2 (ASTM 1995) for determination of flexural properties.

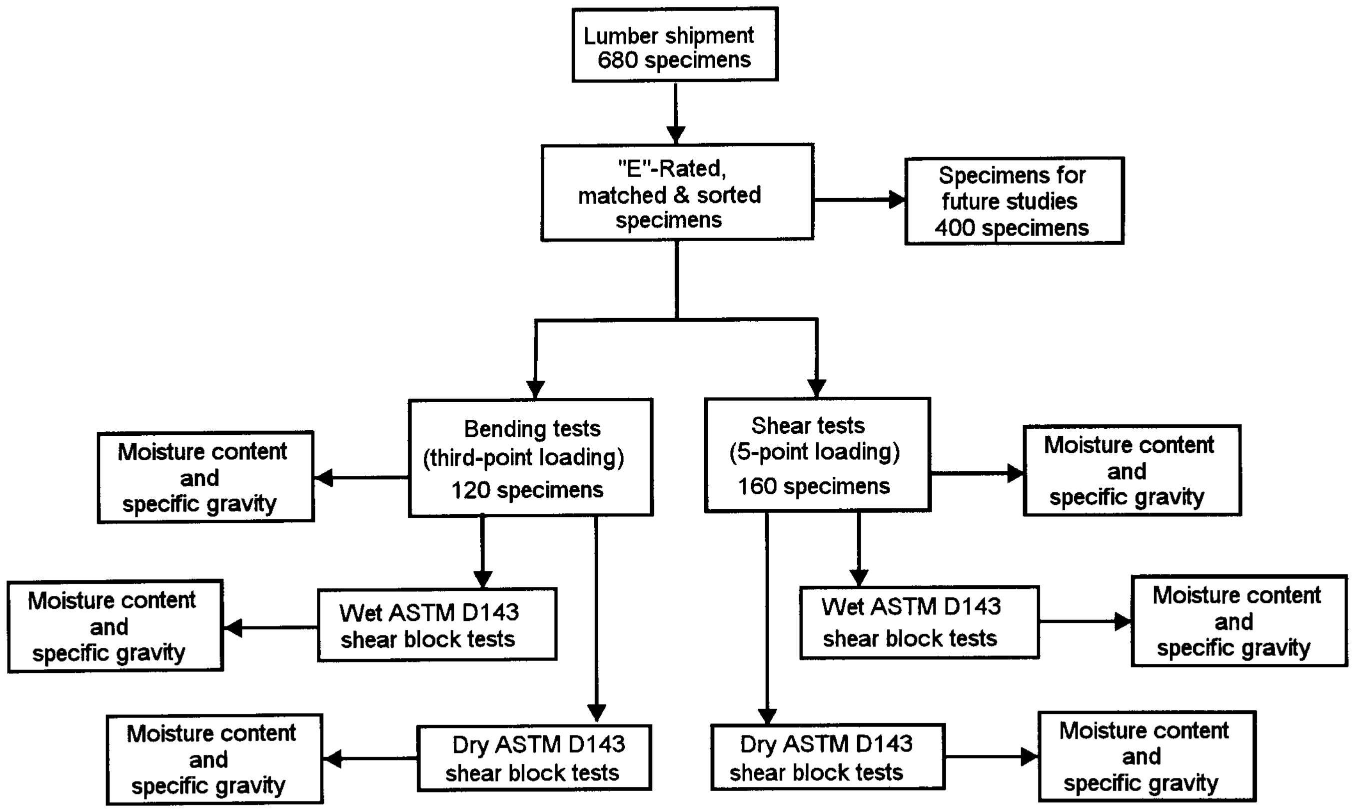

Figure 3—Flowchart of testing program.

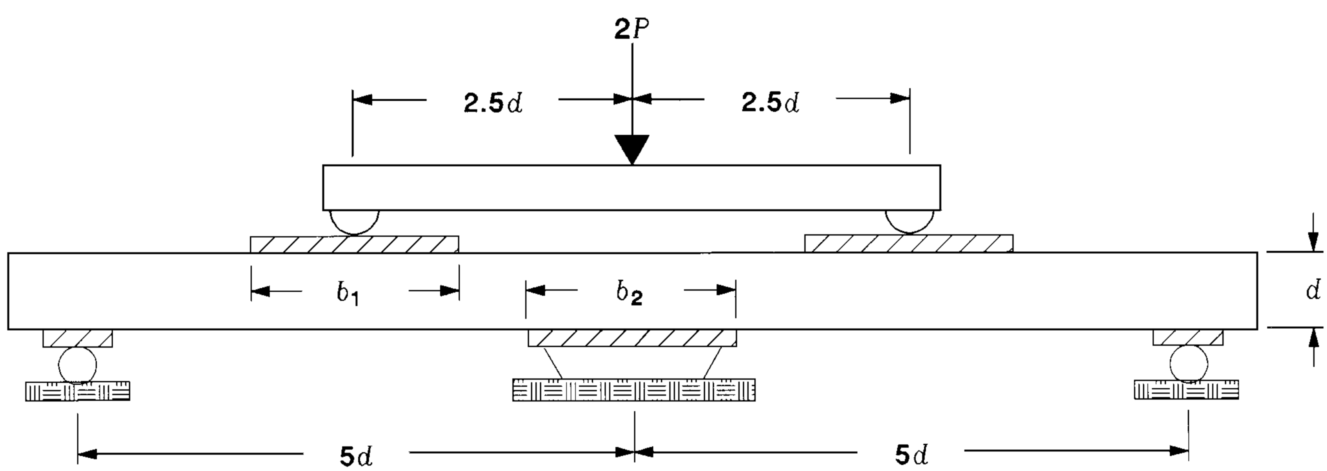

Figure 4—Configuration for five-point loaded beam shear test.

Table 2—Setup dimensions for five-point loading beam shear test

Beam size	Span length (in. (m)) 2.5*d*	5*d*	Plate length (in. (mm)) b_1	b_2
2 by 4	$8^3/_4$ (0.22)	$17^1/_2$ (0.44)	6 (152)	8 (203)
2 by 10	$23^1/_8$ (0.59)	$46^1/_4$ (1.18)	12 (305)	15 (45)
4 by 8	20 (0.51)	40 (1.02)	10 (254)	12 (305)
4 by 12	$29^3/_8$ (0.75)	$58^3/_4$ (1.49)	12 (305)	15 (45)
4 by 14	$34^5/_8$ (0.88)	$69^1/_4$ (1.76)	15 (381)	20 (508)

Failure Definition

A monotonic load was applied until failure in both bending and shear tests. This load was applied at a rate that conforms to ASTM D198 (ASTM 1995), which specifies maximum load to be attained between 6 and 20 min, with failure ideally occurring at 10 min.

Specimens tested for shear strength failed in one of three modes: bending caused by tensile rupture or compressive wrinkles, shear, or compression perpendicular to grain. Some beam shear tests were stopped before reaching any of these failure states because specimens had rotated in the test setup to cause an unstable test configuration. In this case, the maximum load before stopping the test was recorded for data analysis and the specimen was not retested.

Measurements

Measurements included specimen size, weight, moisture content, specific gravity, and maximum load at failure; bending tests also included midspan deflection. Width and depth dimensions were measured to the nearest 0.01in. (0.25 mm) at loading points before testing. Specimens were tested in green condition to reduce the occurrence of any checks or splits. Moisture content readings were taken by two methods. For the first method, a two-pin conductance electronic moisture meter (ASTM 1995) was used at three locations within the failure zone but away from the loading points. For the beam shear specimens, an additional two electronic moisture readings were taken above and below the shear failure in a portion cut from the interior of the cross section. The electronic moisture meter gives results to 30 percent moisture content, which was sometimes lower than the moisture content of the specimens. The second method was to cut small samples from the entire cross-section of the beam and dry them in a oven according to ASTM D4442 for moisture content and ASTM D2395 for specific gravity (ASTM 1995).

Two types of screw-driven machines with different load-measuring sensitivities were used, corresponding to estimated failure loads. The 4 by 14 and 4 by 12 specimens were tested with a 1×10^6 lb (4.45-MN) capacity machine. The remaining specimens were tested with a 175×10^3 lb (779 kN) capacity machine. Load cell accuracies and loading rates for all tests are listed in Table 4.

Deflection measurements were recorded by two methods for the bending specimens. For all sizes except the 2 by 4 beams, deflections were measured within the shear-free zone by a device that was placed on top of the beam and is similar to the middle ordinate deflectometer in ASTM D3043 (ASTM 1995). More detail about the deflection measuring procedures is provided in Appendix A. For 2 by 4 specimens, a yolk supported at the neutral axis was used to measure the midspan deflection relative to the end of the beam

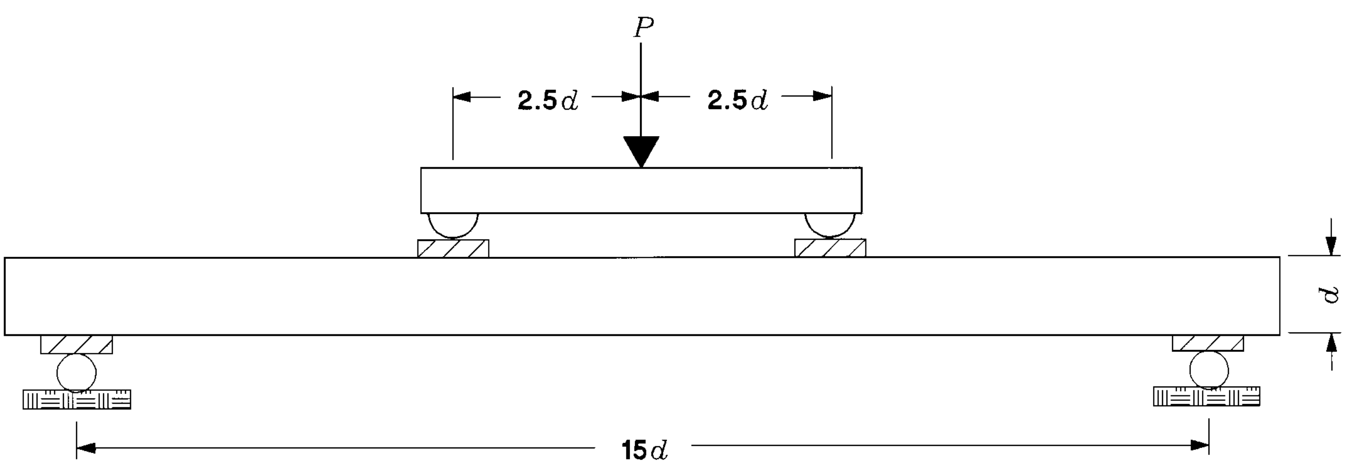

Figure 5—Configuration for third-point bending test.

Table 3—Setup dimensions for third-point bending test

Beam size	Span length (in. (m)) 2.5*d*	15*d*
2 by 4	$8^3/_4$ (0.22)	$52^1/_2$ (1.33)
2 by 10	$23^1/_8$ (0.59)	$138^3/_4$ (3.52)
4 by 8	$18^2/_3$ (0.47)	112 (2.84)
4 by 12	$29^3/_8$ (0.75)	$176^1/_4$ (4.48)
4 by 14	$34^3/_8$ (0.88)	$206^1/_4$ (5.23)

with a linear variable differential transducer (LVDT) with a computerized acquisition system. In both methods, deflections were read at 1-s intervals until failure.

Shear Block Tests

From each beam, two ASTM shear block specimens were cut from undamaged sections adjacent to each other and near the failure. One shear block was tested in the green condition, and the other was tested after conditioning to 12 percent moisture content. Testing procedures conformed to ASTM D143, with the specimen cut along the grain of the material (ASTM 1995). After testing, moisture content (ASTM D4442) and specific gravity (method A, ASTM D2395) were determined from the broken shear block specimens (ASTM 1995).

Analysis

Analytical procedures consisted of maximum stress and elastic modulus calculations, adjustments for moisture content and specific gravity, and censored statistics calculations.

Maximum Stress Calculations

Five-Point Bending

Shear strength values were determined by idealizing the five-point bending test as a single-span beam with one end fixed and the other hinged, with the span length equal to the center-to-center support distance. Shear cracks were typically observed within the middle quarter of the beam depth. Therefore, a parabolic shear stress distribution was assumed. This assumption allows calculation of shear stresses based on techniques consistent with current NDS design specifications (AF&PA 1991).

Based on elementary strength of material principles, the equation for maximum shear stress, in a beam fixed at one end and simply supported at the other end, under the action of a concentrated load at midspan is

$$\tau = \frac{33}{32}\frac{P}{bd} \tag{4}$$

where

- τ is shear stress (lb/in^2 (Pa)),
- P load applied to one span, half the total measured load (lb (N)),
- b beam width (in. (m)), and
- d beam depth (in. (m)).

The load measured is the sum of the load applied at midspan of each span of length 5*d*.

Third-Point Bending

Modulus of rupture values were calculated using beam theory, considering only the load applied to the specimen

Table 4—Test loading rates and load cell accuracy

Beam size	Shear tests: Load rate in/min (mm/min)	Shear tests: Load accuracy lb (N)	Shear tests: Sensitivity[a] (%)	Bending tests: Load rate in/min (mm/min)	Bending tests: Load accuracy lb (N)	Bending tests: Sensitivity[a] (%)
2 by 4	0.04 (1.0)	10 (44)	0.1	0.15 (3.8)	10 (44)	0.1
2 by 10	0.08 (2.0)	10 (44)	0.1	0.15 (3.8)	10 (44)	0.1
4 by 8	0.09 (2.4)	200 (890)	0.2	0.10 (2.5)	10 (44)	0.1
4 by 12	0.11 (2.8)	200 (890)	0.2	0.30 (7.6)	50 (222)	0.1
4 by 14	0.13 (3.3)	200 (890)	0.2	0.40 (10.2)	50 (222)	0.1

[a]Percentage of load accuracy divided by maximum load.

and neglecting the dead weight of the beam. The maximum stress at failure or modulus of rupture is

$$\sigma = \frac{PL}{bd^2} \tag{5}$$

where

σ is flexural stress (lb/in^2 (Pa)),
P total load applied to test setup (lb (N)), and
L span length (in. (m)).

Elastic Modulus Calculations

Two techniques were used to determine the modulus of elasticity. Both shear and bending specimens were nondestructively evaluated by stress wave techniques upon arrival at the Forest Products Laboratory. In addition, bending specimens were instrumented during testing to produce a load versus displacement plot for calculating modulus of elasticity. Equations for each method are outlined in the following section.

Stress Wave of Shear Specimens

Stress wave testing is based upon propagation of compression waves in an elastic material. An impact from a hammer induces a compression wave in the member. The time required for the compression wave to travel from one end of the beam to the other and back is measured by an oscilloscope (Ross and Pellerin 1991,1994). Beam weight was measured with a spring balance prior to testing. Weight of each specimen was determined to the nearest pound for 4 by 8 and larger specimens and to the nearest half-pound for the remainder of the specimens. With this information, the elastic modulus of the beam was determined from

$$E_{sw} = C^2 \rho \tag{6}$$

where

E_{SW} is stress wave elastic modulus (lb/in^2 (Pa)),
C compression wave speed (in/s (N/m)), and
ρ mass density of specimen (lbm/in^3 (kg/m^3)).

Moisture content of each specimen was measured with a two-pin conductance electronic moisture meter (ASTM 1995) to the nearest percentage up to 30 percent. Stress-wave elastic values for all beam shear specimens are listed in Appendix B.

Load and Deflection of Bending Specimens

Load and deflection measurements were continuously recorded while the beams were loaded to failure according to ASTM D198 (1995) test procedures. Elastic modulus values were calculated by linear regression of the load versus deflection data between 20 and 40 percent of the maximum load at failure. For all specimens except the 2 by 4 specimens, deflections were measured in the shear-free section of the beam and were calculated with the following expression:

$$E = \left(\frac{P}{\Delta}\right)\frac{3Ls^2}{4bd} \tag{7}$$

where

E is elastic modulus (lb/in^2 (Pa)),
L beam span (in. (m)),
s span length of test device (in. (m)), and
Δ midspan deflection (in. (m)).

Details of the experimental parameters for measuring elastic modulus are given in Appendix A. For the 2 by 4 specimens, deflections were measured relative to the neutral axis at each end of the beam and thus included a component of shear deformation. To account for shear deformation, the following expression for modulus of elasticity was used:

$$E = \frac{PL^3}{4.7bd^3\Delta\left(1 - \frac{PL}{5bdG\Delta}\right)} \tag{8}$$

where the shear modulus G (lb/in^2) is taken to equal 1/16 times the calculated E. This meant that the calculated E was found by iteration. All bending elastic modulus values published in this report are true or "shear free" values (Appendix C).

Moisture Adjustments

ASTM D245 uses a seasoning factor to adjust green ASTM D2555 strength values to defined dry conditions for lumber. For solid-sawn lumber, dry is defined as an average moisture content of 15 percent with a maximum of 19 percent moisture content (ASTM D245); for glued-laminated timber products, dry is defined as an average moisture content of 12 percent with a maximum of 16 percent moisture content (ASTM D3737) (ASTM 1995). Dry/green ratios for adjusting green, clear straight-grain wood strength values to 12 percent moisture content for many clear wood species are given in ASTM D2555. Although ASTM D245 and ASTM D2555 provide procedures for adjusting strength values from green to a defined dry condition, these standards lack procedures for adjusting strength values from any moisture content other than green.

ASTM D2915 outlines a procedure for adjusting shear strength for varying moisture conditions with green defined as 22 percent moisture content, but advises that the expression not be used for adjustments that are more than 5 percentage points of moisture content. The following equation is the ASTM D2915 expression for adjusting shear strength for moisture content:

$$P_2 = P_1\left(\frac{1.33 - 0.0167M_2}{1.33 - 0.0167M_1}\right) \tag{9}$$

where

P_1 is shear strength at moisture content M_1, and
P_2 shear strength adjusted to moisture content M_2.

In addition to ASTM procedures, the following exponential formula for adjusting strength values at moisture contents other than green or dry was proposed by Wilson (1932):

$$\log S_3 = \log S_1 + \left(\frac{M_1 - M_3}{M_1 - M_2}\right)\log\frac{S_2}{S_1} \tag{10}$$

where S_i is strength (lb/in^2 (Pa)) at a given moisture content. Equation (10) is to be applied between 9 percent and M_p moisture content. M_p is defined as that moisture content that intersects a horizontal line representing green strength and a line representing logarithmic strength–moisture relationships and is lower than the fiber saturation point. The *Wood Handbook* (Forest Products Laboratory 1987) defines this M_p value as 24 percent for Douglas-fir. In the 1955 edition of the *Wood Handbook*, this expression is rearranged as

$$\log S_3 = \log S_2\,(M_2 - M_3)\left(\frac{\log (S_{12} / S_g)}{M_p - 12}\right) \tag{11}$$

where

S_3 is estimated strength value at M_3 moisture content,
M_3 moisture content at which estimated strength is desired,
S_2 known strength at moisture content M_2,
S_{12}/S_g dry/green ratio for strength property of interest, and
M_p intersection moisture content (percent),

which gives a good estimate of the strength value with known dry/green ratios. The specific moisture adjustment used will be noted before each calculation.

Specific Gravity Adjustments

Table 1 of ASTM D2555 (ASTM 1995) currently specifies an average green clear wood specific gravity of 0.45 for coast and interior north Douglas-fir, 0.46 for interior west Douglas-fir, and 0.43 for south Douglas-fir. In our tests, the specific gravity values of bending and shear test specimens were different than these standardized values. Adjustments derived from ASTM shear blocks were applied to account for differences in strength from specific gravity. Specific gravity adjustments for green Douglas-fir species are found in the Western Wood Density Survey (Forest Products Laboratory 1965). These adjustments consist of linear equations for the four U.S. regions of Douglas-fir; the coefficients of the linear expressions are listed in Table 5. These adjustments are used to normalize the data to a specific gravity of 0.45 when noted.

Table 5—Coefficients of linear regression for green shear strength as function of specific gravity[a]

Douglas-fir species	Intercept (lb/in^2) (MPa)	Slope (lb/in^2/SG) (MPa)
Coast	193 (1.33)	1,580 (10.89)
Interior west	174 (1.20)	1,699 (11.71)
Interior north	184 (1.27)	1,711 (11.80)
Interior south	18 (0.24)	2,171 (14.97)

[a]Western Wood Density Survey (1965). SG is specific gravity.

Censored Statistics Calculations

Beam shear specimens are expected to have failure modes other than shear, based on the results of Rammer and Soltis (1994) and Leicester and Breitinger (1992). Information from suspended shear tests can still be used to calculate means and standard deviations. The following are the expressions for the maximum likelihood estimators (MLEs) that take censored data sets into consideration.

The MLE procedure uses the following expressions and techniques as described in Lawless (1982), exploiting the relationship that if shear strength distribution is lognormal, log shear strength is normally distributed. The likelihood function[1] is expressed as:

$$L(\mu,\sigma) = \prod_{i\in D}\frac{1}{\sigma}\phi\left(\frac{y_i-\mu}{\sigma}\right)\prod_{i\in C}Q\left(\frac{y_i-\mu}{\sigma}\right) \tag{12}$$

where μ and σ are the true population mean and standard deviation of the normal distribution, respectively; ϕ and Q are expressions of the standard normal probability density and survivor functions (one minus cumulative distribution function), respectively; D is the set of specimens for which y_i is the observed log shear strength; and C is the set of specimens for which y_i is the observed log censored shear strength. Expressions of the standard normal density and survivor functions are as follow:

$$\phi\left(\frac{y_i-\mu}{\sigma}\right) = \frac{1}{\sqrt{2\pi}}e^{-[(y_i-\mu)/\sigma]^2/2} \tag{13}$$

$$Q\left(\frac{y_i-\mu}{\sigma}\right) = \int_{\left[\frac{y_i-\mu}{\sigma}\right]}^{\infty}\phi(x)\,dx \tag{14}$$

[1] $\prod$ is defined as the range of products, which means $\prod_{i=1}^{n} a_i = a_1 a_2 \ldots a_n$.

Substituting ϕ and Q into Equation (12) and taking the logarithm of the expression results in the log likelihood function

$$\log L(\mu, \sigma) = -r \log \sigma - \frac{1}{2\sigma^2} \sum_{i \in D} (y_i - \mu)^2 + \sum_{i \in C} \log Q\left(\frac{y_i - \mu}{\sigma}\right) + \frac{r}{2} \log(2\pi) \tag{15}$$

where r is the number of observed uncensored shear strengths. Estimates of the mean and standard deviation are determined by maximizing the log likelihood function. Maximize Equation (15) by taking derivatives with respect to both σ and μ and setting each expression to zero. This leads to the following system of equations:

$$\sum_{i \in D} z_i + \sum_{i \in C} V(z_i) = 0 \tag{16}$$

$$-r + \sum_{i \in D} z_i^2 + \sum_{i \in C} z_i V(z_i) = 0 \tag{17}$$

where $V(z_i)$ is the hazard function of the normal distribution, $\phi(z_i)/Q(z_i)$, and $z_i = (y_i - \mu)/\sigma$. Estimates of the mean and standard deviation, $\hat{\mu}$ and $\hat{\sigma}$, are determined by an iterative process using Equations (16) and (17). Approximate standard errors of the estimated mean and variance are determined by inverting the Fisher information matrix $\mathbf{I}_o$ (Eq. (18)).

$$\mathbf{I}_o = \begin{pmatrix} \dfrac{-\partial^2 \log L}{\partial \mu^2} & \dfrac{-\partial^2 \log L}{\partial \mu \, \partial \sigma} \\ \dfrac{-\partial^2 \log L}{\partial \mu \, \partial \sigma} & \dfrac{-\partial^2 \log L}{\partial \sigma^2} \end{pmatrix}_{(\hat{\mu}, \hat{\sigma})} \quad 18)$$

where $\log L$ is the log likelihood function in Equation (15). The square root of the diagonal entries of the inverted matrix are approximate standard errors for $\hat{\mu}$ and $\hat{\sigma}$. This procedure determines the maximum likelihood estimates of mean and standard deviations of the normal distributed log shear stress, $\hat{\mu}$ and $\hat{\sigma}$.

For comparison with experimental observations, the following expressions were used to calculate the lognormal mean and standard deviations, $\hat{\mu}_\ell$ and $\hat{\sigma}_\ell$, which are one-to-one functions of the estimates $\hat{\mu}$ and $\hat{\sigma}$:

$$\hat{\mu}_\ell = \tilde{\mu} e^{\hat{\sigma}^2/2} \tag{19}$$

$$\hat{\sigma}_\ell = \tilde{\mu}(e^{2\hat{\sigma}^2} - e^{\hat{\sigma}^2})^{1/2} \tag{20}$$

where $\tilde{\mu} = e^{\hat{\mu}}$ (estimated median value of strength). These expressions, Equations (12) through (20), are used to estimate censored data set means and standard deviations.

Results

Average values and coefficients of variation for beam shear, flexural strength, and shear block specimens are summarized in Tables 6 through 9. Data for individual Douglas-fir beam shear and bending specimens are presented in Appendixes B and C, respectively.

Shear Tests

Five-point bending tests resulted in 99 shear failures out of 160 specimens tested—a 62-percent shear failure rate. Table 6 lists the average shear strength values and coefficients of variation of only those specimens that failed in shear, along with the shear stress at failure regardless of failure mode for each beam size tested. Shear strength and shear stress at failure were approximately equal for beam sizes that had a high percentage of shear failures. For the 2 by 4 and 2 by 10 specimens with a lower percentage of shear failures, shear strength and shear stress at failure were different, possibly indicating that the true average shear strength is higher. The coefficient of variation values for solid-sawn Douglas-fir shear strength reported here—11.5 to 17.9 percent—are greater than the 8-percent values observed in glued-laminated Douglas-fir beams (Rammer and Soltis 1994). Cumulative distributions of shear strength for each beam size, including specimens that failed in modes other than shear, are shown in Figure 6. Results shown were not adjusted for moisture content or specific gravity. Detailed information for each specimen is given in Appendix B.

Bending Tests

Most of the 120 beams tested in bending failed either in tension or compression parallel to the grain. The type of beam failure for each specimen is described in Appendix C. Average modulus of rupture, coefficient of variation, and average moisture content for each beam size are shown in Table 7. Cumulative distributions of the modulus of rupture for each beam size are shown in Figure 7; the data were not adjusted to a reference moisture or specific gravity. During bending tests of 4 by 8 specimens, one specimen failed by shear at an existing check.

Shear Block Tests

Two shear block specimens were cut from each beam test specimen regardless of failure mode. One shear block specimen was tested at approximately the same moisture content as that of the beam at the time of testing; the other

Table 6—Douglas-fir beam shear strength results

Beam size	Shear failures/ total tests	Moisture content (%)	Shear strength lb/in^2 (MPa)	COV[a] (%)	Shear stress at failure lb/in^2 (MPa)	COV (%)
2 by 4	24/40	20.9	1,440 (9.92)	11.5	1,370 (9.45)	13.4
2 by 10	11/40	21.7	973 (6.71)	16.8	921 (6.35)	16.2
4 by 8	30/40	24.6	870 (5.99)	13.2	860 (5.92)	13.8
4 by 12	17/20	24.6	750 (5.02)	17.9	750 (5.15)	18.8
4 by 14	17/20	23.9	730 (5.01)	12.7	740 (5.10)	12.8

[a]COV is coefficient of variation.

Table 7—Douglas-fir bending strength results

Beam size	Number of tests	Average moisture content (%)	Modulus of rupture lb/in^2 (MPa)	COV (%)
2 by 4	40	20.2	6,250 (43.1)	23.2
2 by 10	20	20.4	3,380 (23.3)	27.1
4 by 8	20	23.8	4,500 (31.0)	28.8
4 by 12	20	23.1	3,610 (24.9)	31.8
4 by 14	20	19.8	4,050 (28.0)	41.2

Table 8—ASTM shear block strength test results

Condition	Beam size	Number of tests	Specific gravity[a]	COV	Moisture content (%)	Shear strength lb/in^2 (MPa)	Shear strength COV[b] (%)
Green	2 by 4	40	0.43	13.7	21.2	1,090 (7.49)	18.3
	2 by 10	40	0.40	10.9	25.7	920 (6.32)	21.1
	4 by 8	40	0.44	13.1	28.0	970 (6.70)	21.8
	4 by 12	20	0.46	11.3	28.1	1,040 (7.19)	15.7
	4 by 14	20	0.43	8.5	25.9	980 (6.78)	10.4
	Wood Handbook[b]		0.45[c]	—	—	900 (6.21)	14
			0.45[d]	—	—	950 (6.55)	—
Dry	2 by 4	40	0.46	13.1	11.0	1,620 (11.2)	16.0
	2 by 10	39	0.45	11.2	10.6	1,450 (10.0)	13.6
	4 by 8	40	0.46	13.8	11.0	1,600 (11.0)	15.4
	4 by 12	20	0.49	14.7	11.4	1,530 (10.6)	16.0
	4 by 14	19	0.45	10.2	10.8	1,450 (9.99)	15.0
	Wood Handbook		0.48[c]	—	—	1,130 (7.79)	14
			0.48[d]	—	—	1,400 (9.65)	—

[a]Based on ovendry weight divided by wet volume.

[b]Forest Products Laboratory (1987).

[c]Coast Douglas-fir.

[d]Interior north Douglas-fir.

Table 9—ASTM shear block third-point bending test results

Condition	Beam size	Number of tests	Specific gravity[a]	COV	Moisture content (%)	Shear strength lb/in² (MPa)	Shear strength COV (%)
Green	2 by 4	40	0.43	12.7	24.3	960 (6.60)	17.8
	2 by 10	20	0.40	14.2	22.5	970 (6.70)	19.3
	4 by 8	20	0.44	11.6	31.1	990 (6.83)	12.8
	4 by 12	20	0.41	8.7	27.6	910 (6.28)	14.2
	4 by 14	20	0.45	11.7	19.5	1,110 (7.66)	23.1
	Wood Handbook[b]		0.45[c]	—	—	900 (6.21)	14
			0.45[d]	—	—	950 (6.55)	—
Dry	2 by 4	40	0.45	16.1	10.6	1,630 (11.2)	18.8
	2 by 10	19	0.42	13.6	10.8	1,420 (9.77)	18.7
	4 by 8	20	0.46	12.3	11.1	1,590 (10.0)	16.9
	4 by 12	20	0.43	12.2	11.0	1,390 (9.56)	17.9
	4 by 14	20	0.48	13.0	11.2	1,560 (10.6)	12.7
	Wood Handbook		0.48[c]	—	—	1,130 (7.79)	14
			0.48[d]	—	—	1,400 (9.65)	—

[a]Based on ovendry weight divided by wet volume.
[b]Forest Products Laboratory (1987).
[c]Coast Douglas-fir.
[d]Interior north Douglas-fir.

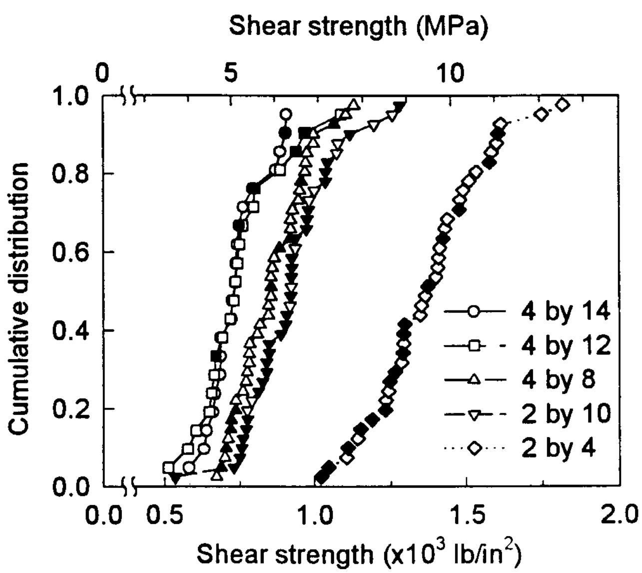

Figure 6—Cumulative distribution of Douglas-fir beam shear strength for various beam sizes. Solid symbols indicate shear stress attained during nonshear failure mode.

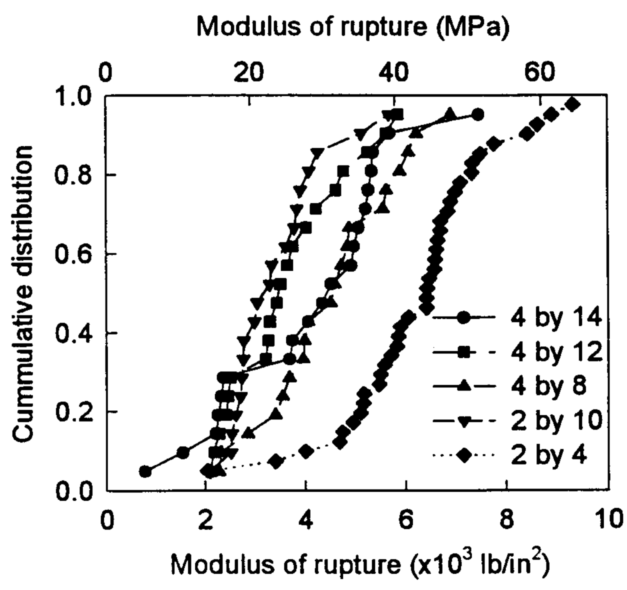

Figure 7—Cumulative distribution of Douglas-fir modulus of rupture for various beam sizes.

shear block specimen was dried to about 12 percent moisture content before testing. Average values and coefficients of variation for green and dry shear blocks are listed in Tables 8 and 9. Cumulative distribution of shear block data is shown in Figure 8. The values for green shear blocks were similar to published average strength and variability (Forest Products Laboratory 1987, ASTM 1995). The strength values for dry shear blocks, however, were greater than the published values of 1,130 to 1,510 lb/in^2 (7.8 to 10.4 MPa) (Forest Products Laboratory 1987). However, the variation was similar to accepted levels. High dry shear strength values resulted in an experimental dry/green ratio greater than the ASTM D2555 dry/green ratio (Table 10). Specific gravity results (ovendry weight/green volume) were within the typical 1,130 to 1,510 lb/in^2 (7.8 to 10.4 MPa) range for coast Douglas-fir (0.48).

Discussion

The five-point bending test procedure produced 99 shear failures in 160 tests, resulting in a 62-percent success rate. Of the 61 specimens that did not fail in shear, 52 failed in bending and 9 had excessive compression under loading points or problems with stability. The lowest level of success occurred in the 2 by 10 specimens. These specimens experienced a high incidence of bending failures, which was attributed to lower than average modulus of rupture. The average modulus of rupture of the 2 by 10 specimens was 16 percent lower than the in-grade average of 4,040 lb/in^2 (27.9 MPa) for this beam size at 23 percent moisture content (Evans and Green 1987). Other types of failure observed in the 2 by 10 specimens were local buckling and compression. A smaller aspect ratio (beam height divided by width) should also reduce the problem of local and lateral stability in future tests.

In general, shear failures started in the wood at the highly stressed region between the load supports and rarely propagated past the loading points (Fig. 9). Shear failures were observed in a five-point bending test by the relative longitudinal displacement of vertical lines drawn prior to testing. In this test, cracks propagate from the highly shear stressed middle half of the beam and continue until there is a reduction in shear stress, near the loading points. In our tests, the cracks did not propagate to the end of the beam, and thus failure could not be identified by visible end-displacement. A substantial load reduction was always noted at crack initiation. In some cases, a sustained load after shear failure produced a bending failure. This is reasonable because after failing in shear, the cross-sectional moment of inertia is reduced by about 75 percent; therefore, even with a reduction in load after cracking, the remaining cross-section could fail in bending.

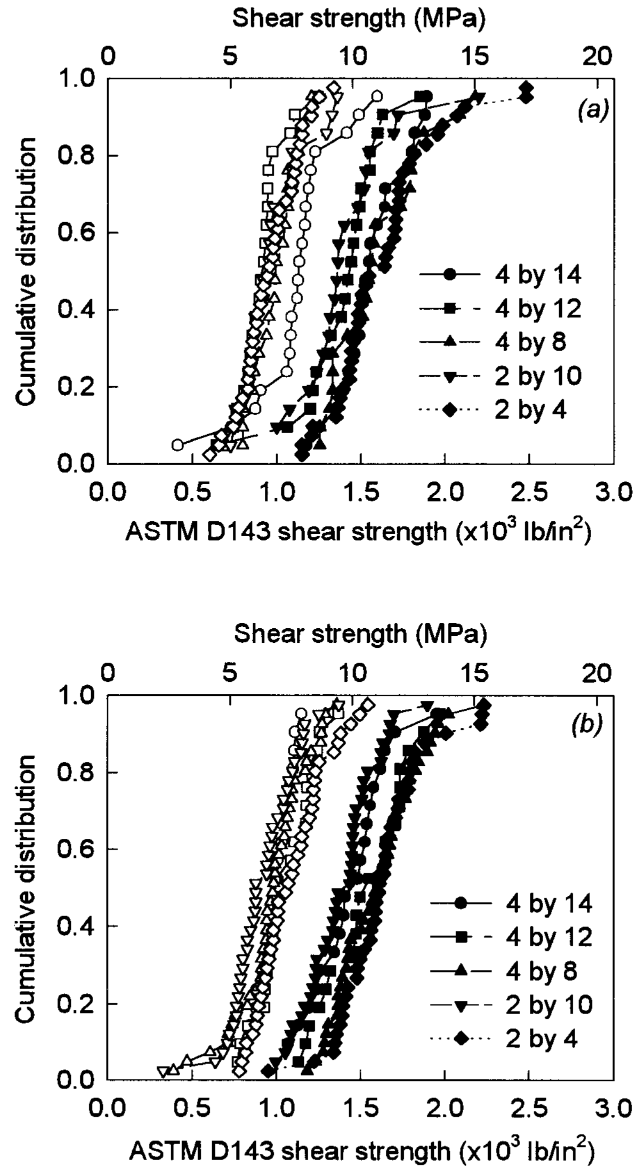

Figure 8—Cumulative distribution of Douglas-fir ASTM shear block strengths: (a) shear blocks obtained from original beam shear specimens; (b) shear blocks obtained from original bending specimens. Open symbols indicate shear strength values at moisture content of original specimen. Solid symbols indicate shear strength values of dry specimens.

Table 10—ASTM D2555 dry/green ratios for Douglas-fir

Douglas-fir species	Modulus of rupture	Modulus of elasticity	Shear strength
Coast	1.62	1.25	1.38
Interior west	1.64	1.21	1.59
Interior north	1.76	1.27	1.48
Interior south	1.75	1.28	1.59

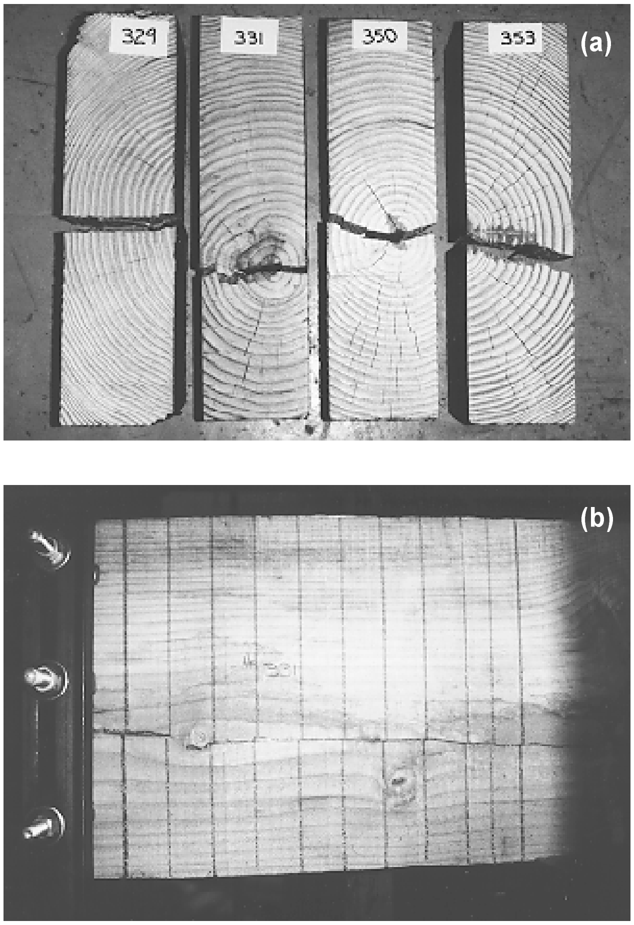

Figure 9—Shear failures observed during testing: (a) cross-sectional view of beam; (b) side view of beam.

Overall, using a five-point loading configuration to evaluate shear strength of unsplit Douglas-fir beams is an acceptable method for producing shear failures provided that care is taken to select beams with small aspect ratios and to obtain material with adequate bending strength. In addition, the five-point configuration is representative of actual continuous beam applications where critical shear stress conditions exist. In our tests, experimental beam shear strength coefficients of variation averaged 14.2 percent. The coefficients of variation are slightly higher than values observed for glued-laminated beams (Rammer and Soltis 1994) and the same as the shear block strength values published in ASTM D2555 for Douglas-fir.

Experimental shear block coefficients of variation ranged from 12.7 to 18.8 percent for dry specimens and 10.4 to 23.1 percent for green specimens. The average variation was 16.1 percent for dry specimens and 17.5 percent for green specimens. These values are slightly higher than the published coefficient of variation of 14 percent for green material (ASTM 1995). The slightly higher variation for green specimens is likely attributable to the wider range of moisture contents; only 145 of 280 blocks had ≥24 percent moisture content. Overall, the strength variation results are consistent with published values.

Dry/Green Ratio and Specific Gravity–Shear Strength Relationship

An experimental dry/green ratio for shear blocks was compared to published ASTM ratios for all Douglas-fir classification. Only 145 matched green shear blocks with moisture content greater than M_p (24 percent moisture content) were considered. The average dry/green ratio of the matched specimens was 1.69 at an average dry moisture content of 10.9 percent. Using the Wilson logarithmic expression (Eq. (10)) to adjust individual dry strength values to 12 percent moisture content resulted in a dry/green ratio of 1.61 with a coefficient of variation of 20.7 percent. This value is greater than the published ASTM D2555 value for coast Douglas-fir (Table 10). Confidence intervals (CIs) for the dry/green ratio were calculated by the delta method (Mood and others 1974), which gives Taylor series approximations of the mean and its standard error. Accordingly, an approximate 100(1 – α) percent two-sided CI is calculated as

$$\mathrm{CI} = (\mathrm{Dry} / \mathrm{Green}) \pm z_{\alpha/2} \cdot \mathrm{SE}_{\mathrm{Dry/Green}} \qquad (21)$$

where $z_{\alpha/2}$ = 100α/2 percentile point of standard normal variate and SE is standard error of dry/green ratio.

The delta method resulted in a dry/green estimate of 1.608, with a standard error of 0.024. The 99-percent dry/green ratio CI using (Eq. (21)) is (1.55,1.67), indicating that the ratio does not vary to a great extent.

The relationship of ASTM shear block strength to moisture content was plotted to indicate which moisture adjustment procedure, ASTM 2915 (ASTM 1995) or Wilson's method (Wilson 1932), better modeled the mean of our data (Fig. 10). Wilson's expression was plotted using M_p = 24 percent and a dry/green ratio of 1.61. The ASTM D2915 procedure was plotted using M_1 = 22 percent. Data from shear block specimens with moisture content greater than the fiber saturation level were plotted at 30 percent moisture content. Clearly, Wilson's expression gave a better fit for the shear block data; it was used to adjust beam shear data for moisture content where noted.

The relationship between specific gravity G and shear strength τ was also established for the 145 ASTM shear block specimens with moisture content ≥24 percent. A linear regression resulted in the following expression:

$$\tau = 88.6 + 1{,}962G \qquad (22)$$

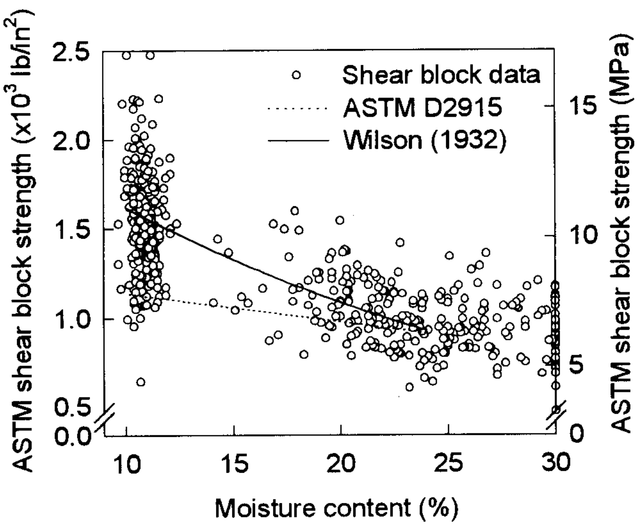

Figure 10—Relationship of ASTM shear strength to moisture content. Lines represent published expressions to adjust shear strength values for moisture content. (Note: shear blocks with moisture content greater than 30 percent were plotted at 30-percent level.)

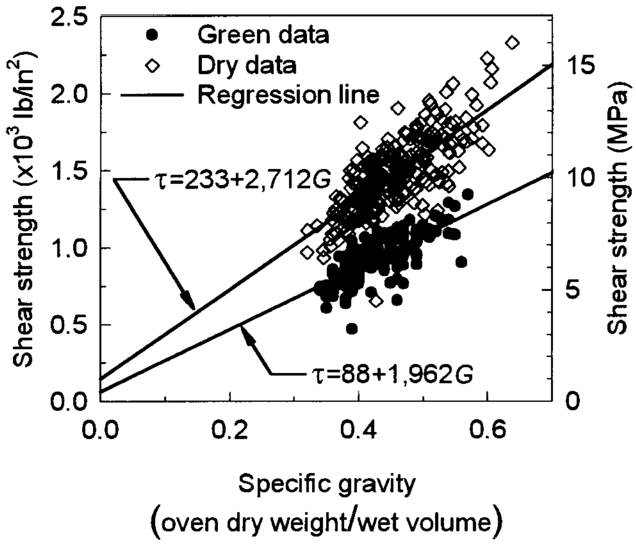

Figure 11—Regression of specific gravity and ASTM shear strength at 12 and 24 percent moisture content. Top regression line represents results from dry specimens, bottom line from green specimens.

with a coefficient of determination $r^2 = 0.40$ and a standard error estimate of 125.0. This expression is similar to that expressed in the Western Wood Density Survey (Forest Products Laboratory 1965, Table 5), but with a lower coefficient of determination and similar standard error estimate. In addition, a linear regression of the 280 dry shear block specimens at an adjusted 12-percent moisture content resulted in the following relationship between specific gravity and shear strength:

$$\tau = 233 + 2{,}712G \tag{23}$$

with $r^2 = 0.49$ and an error estimate of 170.4. Equations (22) and (23) and the data are plotted in Figure 11. Equations (22) and (23) are used to adjust beam shear for specific gravity where noted.

Shear Strength to Beam Size Relationship

A plot of unadjusted shear strength as a function of shear area indicates a general increase of shear strength with smaller area (Fig. 12). The 2 by 10 beams were somewhat lower in strength than expected because of the high incidence of different failure modes, resulting in an extremely censored data set. Thus, the censoring effect needed to be taken into consideration in data analysis.

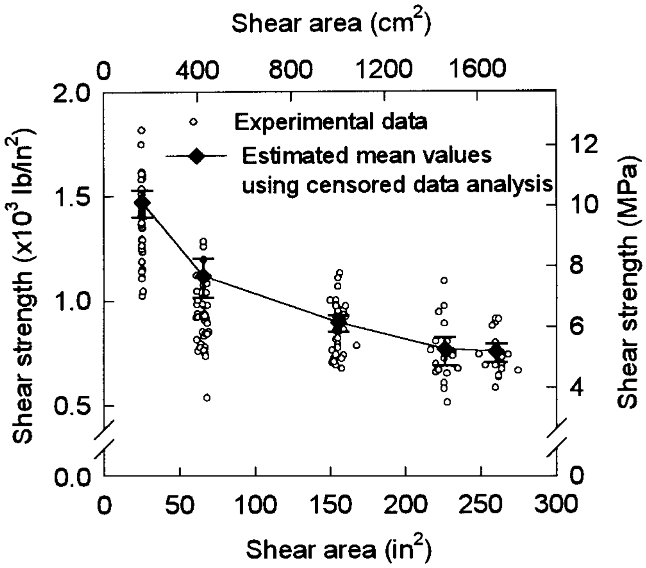

Figure 12—Relationship of beam shear strength to shear area. Experimental values are plotted as open circles. Estimated means and confidence limits, calculated by censored data analysis, are plotted as lines and solid symbols.

Two statistical approaches, a commercial statistical software package (SAS) and a maximum likelihood estimator (MLE) procedure, were used to estimate the uncensored mean and standard deviation of shear strength. The SAS LIFETEST (SAS Institute Inc. 1988) procedure, which assumes a nonparametric distribution and a power curve relationship of the data, predicted higher average values than did the SAS LIFEREG procedure, which assumes various parametric distributions, but both predict estimated mean greater than

Table 11—Maximum likelihood estimates of unadjusted shear strength results

Beam size	$\tilde{\mu}$ (lb/in^2 (MPa))	SE ($\tilde{\mu}$)	Lower 95% (lb/in^2 (MPa))	Upper 95% (lb/in^2 (MPa))	$\hat{\mu}_\ell$ (lb/in^2 (MPa))	COV estimate (%)
2 by 4	1,462 (10.1)	33.4	1,398	1,529	1,473 (10.2)	12.2
2 by 10	1,103 (7.60)	47.8	1,014	1,201	1,118 (7.71)	16.2
4 by 8	886 (6.11)	20.8	846	928	895 (6.17)	13.8
4 by 12	750 (5.17)	34.0	686	820	765 (5.26)	19.9
4 by 14	743 (5.12)	23.5	698	791	752 (5.19)	13.4

Table 12—Likelihood ratio tests for distribution of unadjusted shear strength data

Comparison	T statistic	χ^2 (1-α,2K-2)	p-value	Accept equality hypothesis?
2 by 4 to 2 by 10	31.980	9.210	<0.001	No
2 by 10 to 4 by 8	24.775	9.210	<0.001	No
4 by 8 to 4 by 12	16.020	9.210	<0.001	No
4 by 12 to 4 by 14	2.061	9.210	0.357	Yes

average experimental values. The MLE analysis, described in the Analysis section, also indicated the same trend assuming a lognormal population distribution (Table 11). Since the SAS and the MLE analyses indicated the same higher mean estimates, hereafter the estimates of uncensored data are based solely on the MLE analysis assuming a lognormal distribution. The estimated mean and standard deviation for each beam size are plotted in Figure 12 and listed in Table 11. Overall, the estimated shear strength mean values were higher than the experimental values. The greatest difference between the estimated mean and average experimental shear strength occurred for the highly censored data for the 2 by 10 specimens.

Pairwise likelihood ratio (LR) tests were used to determine if there is a significant difference in the shear strength of beams of different sizes (Nelson 1982). The LR test statistic T is defined as

$$T = 2(\log \mathcal{L}_1 + \ldots + \log \mathcal{L}_K - \log \mathcal{L}_\beta) \qquad (24)$$

where $\mathcal{L}_K$ is the likelihood value of individual size sets using the estimates $\hat{\sigma}$ and $\hat{\mu}$ and $\mathcal{L}_\beta$ is the likelihood value of the combined set, as calculated by Equation (15) using the combined estimates. The statistic is rejected or accepted by comparison with the chi-square distribution with $2K - 2$ degrees of freedom and an assumed level of significance.

The approximate test is

if $T \le \chi^2(1 - \alpha, 2K - 2)$, fail to reject the equality hypothesis,

if $T > \chi^2(1 - \alpha, 2K - 2)$, reject the equality hypothesis,

at a level of significance α. In addition, the p-value is calculated to indicate the smallest level of α at which the data are significantly different. Table 12 lists the pairwise comparisons of the experimental data with a 0.01 level of significance (99 percent level of confidence). For Douglas-fir, there was no statistical difference in distribution of shear strength between the 4 by 12 and 4 by 14 beams. However, the three smaller sizes did show significant differences. Since this LR test simultaneously compares the μ and σ parameters, further comparisons are necessary to determine why differences exist.

Confidence intervals were calculated for the ratios of the scale parameters σ for log strength (Nelson 1982). Based on the scale estimates $\hat{\sigma}$, 95-percent CIs were calculated (Table 13). All CIs included the value of 1, thus the neighboring scale parameters did not differ significantly.

Pairwise LR tests comparing the scale estimates showed similar results (Table 14). In addition, the previous LR tests showed significant differences, with the exception of the 4 by 12 and 4 by 14 data. This suggests differences in the mean log strength values, and hence the mean strength values are the principal cause of strength variation. In fact, approximately 95-percent CIs on the mean log strength differences of neighboring size groups, assuming a common variance (using a linearly pooled estimate), also resulted in the same declared difference as did the LR test for distributional differences. In summary, the LR test revealed a change in shear strength with beam size, with the relationship becoming asymptotic to a constant value for larger beams.

Regression analyses were performed by regressing either beam depth, shear area, or beam volume as a function of

Table 13—Confidence intervals on ratios of scale parameters σ

Comparison	95% confidence interval Lower limit	Upper limit	Does confidence interval include 1?
$\sigma_{2\text{ by }4} / \sigma_{2\text{ by }10}$	0.4692	1.2173	Yes
$\sigma_{2\text{ by }10} / \sigma_{4\text{ by }8}$	0.7376	1.8635	Yes
$\sigma_{4\text{ by }8} / \sigma_{4\text{ by }12}$	0.4528	1.0611	Yes
$\sigma_{4\text{ by }12} / \sigma_{4\text{ by }14}$	0.8807	2.3323	Yes

Table 14—Likelihood ratio tests for scale parameter σ of unadjusted shear strength data

Comparison	*T* statistic	χ^2 (99%,1)	*p*-value	Accept equality hypothesis?
2 by 4 to 2 by 10	1.3968	6.635	0.237	Yes
2 by 10 to 4 by 8	0.2363	6.635	0.627	Yes
4 by 8 to 4 by 12	1.5040	6.635	0.220	Yes
4 by 12 to 4 by 14	1.0295	6.635	0.310	Yes

shear strength. Data were adjusted to a specific gravity of 0.45 and moisture content of 24 percent by the specific gravity and dry/green ratio relationship developed in this report. The adjustments for shear strength were based on local moisture content readings from a two-pin electronic meter and specific gravity measurements observed in the green ASTM shear block. These local values were considered to be more representative of the moisture content and specific gravity at the location of the shear failure than the cross-sectional averages. The regression was performed on the five estimated mean values. Both the coefficient of determination (r^2) (Eq. (25)) and the root mean square residual or error (RMSE) (Eq. (26)) were calculated for several linear and nonlinear expressions to identify which parameter—depth, shear area, or volume—results in the best estimator of shear strength:

$$r^2 = 1 - \frac{\sum (y-\hat{y})^2}{\sum (y-\bar{y})^2} \tag{25}$$

$$\text{RMSE} = \sqrt{\frac{\sum (y-\hat{y})^2}{n}} \tag{26}$$

where

y is observed value,
$\hat{y}$ value predicted using fitted parameters, and
$\bar{y}$ arithmetic mean of sample (Kvålseth 1985).

Table 15—Regressions for relating adjusted green shear strength to beam size[a]

Equation[b]	Independent variable	r^2	RMSE
$y = a + bx$	Depth	0.70	123.0
	Shear area	0.94	51.7
	Volume	0.81	98.6
$y = a + bx + cx^2$	Depth	0.79	122.7
	Shear area	0.99	25.3
	Volume	0.98	31.0
$y = a + b\ln(x)$	Depth	0.68	125.7
	Shear area	0.96	46.1
	Volume	0.89	73.6
$y = ae^{bx}$	Depth	0.70	123.2
	Shear area	0.97	40.0
	Volume	0.85	86.3
$y = ax^b$	Depth	0.66	129.7
	Shear area	0.93	59.7
	Volume	0.85	86.1

[a] r^2 is coefficient of determination; RMSE is root mean square error.
[b] Note: *y* represents shear strength and *x* represents independent variable.

The regression results are given in Table 15. Beam depth *d* was taken as average depth of the beams for a given size. Shear area was taken as average width *b* of the beam multiplied by total length under a maximum shear force action, both positive and negative shear. Beam volume was defined as average width multiplied by average depth multiplied by length of span.

In general, regression analyses indicated higher coefficients of determination using shear area when characterizing the variation of shear strength. Shear strength side effects were modeled well by all the curve equations, which might be attributed to fitting only the estimated mean values rather than all the experimental data.

Previously, Rammer and Soltis (1994) plotted shear area against shear strength for glue-laminated Douglas-fir beam specimens; to relate to the previous study, the following

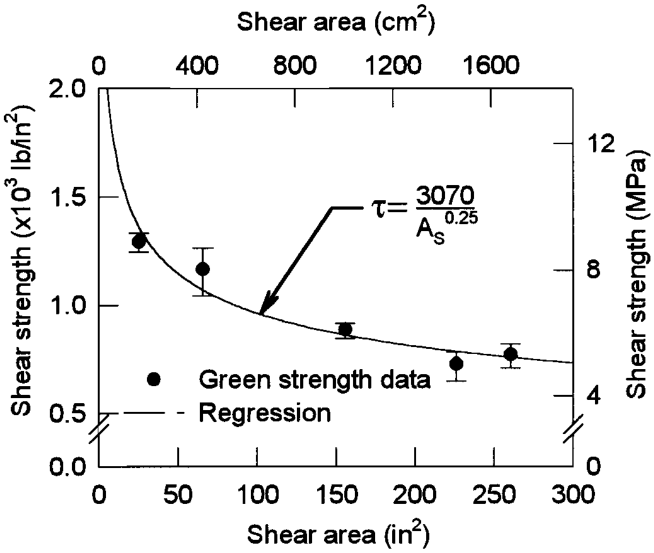

Figure 13—Regression of estimated mean beam shear strength (adjusted to 24 percent moisture content and 0.45 specific gravity) and shear area. Bounds represent 95 percent confidence limits on estimated mean.

discussion focuses on the shear area parameter (Fig. 13). Shear strength decreased with an increase in shear area; the change decreased quickly for small shear areas and asymptotically for larger shear areas. The asymptote resulted in small changes in shear strength for larger beams as was noted in the statistical analysis of the two largest sizes of Douglas-fir beams.

A power curve was regressed independently through the five estimated mean Douglas-fir shear strength values adjusted by the factors developed within this report. The regression equation for Douglas-fir beams is

$$\tau = \frac{3{,}070}{A^{0.25}} \tag{27}$$

where

τ is beam shear strength (lb/in^2) and
A shear area.

The computed coefficient of determination $r^2 = 0.93$ and RMSE = 59.7. Comparing the parameter values with data from previous work on shear of Douglas-fir glued-laminated beams (Rammer and Soltis 1994), the numerator is lower in the work reported here because the results were based on a green condition. However, the exponent, which defines the shape of the curve, on the shear area term is similar. This indicates that the effects of size are similar in glued-laminated and solid-sawn materials.

Table 16—Regressions for relating adjusted green shear strength to shear area, including ASTM shear block

Equation [a]	r^2	RMSE
$y = a + bx$	0.76	204
$y = a + bx + cx^2$	0.89	139
$y = a + b\ln(x)$	0.98	52.4
$y = ae^{bx}$	0.81	202
$y = ax^b$	0.98	58.5

[a] *y* represents shear strength; *x* represents shear area.

Shear Block to Beam Shear Relationship

The effect of stress concentration at the re-entrant corner was discussed by Rammer and Soltis (1994). In summary, the ASTM-assumed shear strength (τ_{ASTM}) is less than the true failure stress (τ_{fail}) by a factor of about 2.0 (Radcliffe and Suddarth 1955). Finite element analysis indicates a factor greater than 2.0, but this analysis did not model effects (crushing and splitting) that might alleviate the stress concentration effect (Cramer and others 1984). Rammer and Soltis (1994) concluded that an estimated stress concentration factor of 2 is appropriate for the ASTM shear block.

When data from beam shear tests were combined with the data from shear block tests, ASTM shear block strength data were adjusted to true maximum stress at failure by

$$\tau_{fail} = C_f \tau_{ASTM} \tag{28}$$

where

C_f is stress concentration factor to adjust ASTM shear block to true stress distribution, assumed to be 2.0, and
τ_{ASTM} ASTM D143 published shear block values.

The adjusted ASTM shear stress τ_{fail} is assumed to occur over a 4-in^2 (64.5-cm^2) failure plane.

A regression analysis of shear area against adjusted green shear strength was conducted, including both the estimated mean beam data and the adjusted mean ASTM shear strength value at the 4-in^2 (64.5-cm^2) shear area (Table 16). The results indicated that the logarithmic and power curve equations modeled shear strength against shear area variation better than did the other models. The forms of these equations are consistent with the prior findings of Longworth (1977) and Rammer and Soltis (1994) on shear strength.

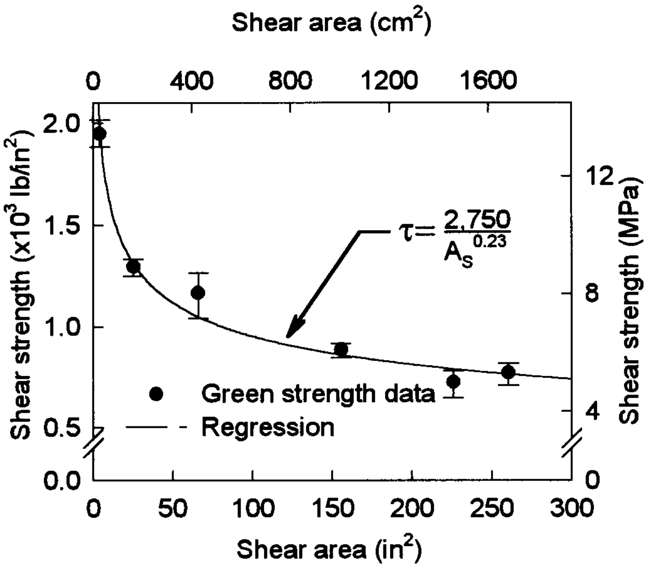

Figure 14—Regression of estimated mean green beam shear strength, including shear block results (adjusted to 24 percent moisture content and 0.45 specific gravity) and shear area. Bounds represent 95 percent confidence limits on estimated mean.

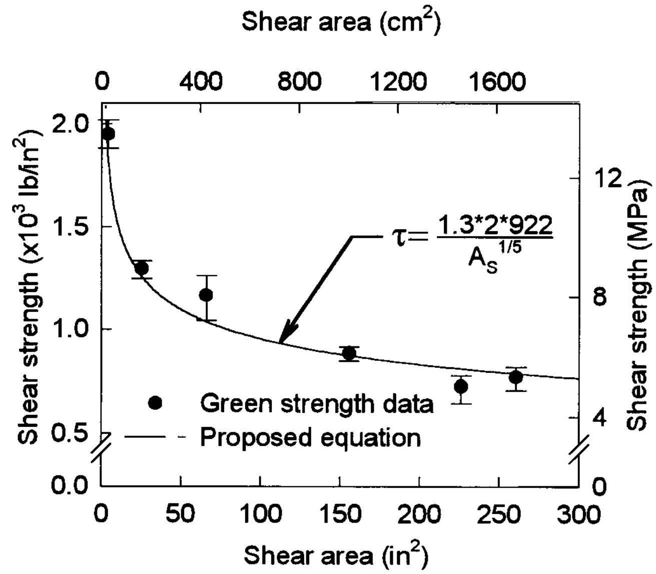

Figure 15—Recommended equation using ASTM D2555 (Table 3) Douglas-fir shear strength value. Bounds represent 95 percent confidence limits on estimated mean of experimental data adjusted to 24 percent moisture content and 0.45 specific gravity.

The τ_{fail} value was plotted with the beam shear data (Fig. 14). A power curve regression, consistent with the finding of the previous beam shear regression analysis, was performed on the combined data set adjusted for specific gravity and moisture content. For Douglas-fir data, the regression equation is

$$\tau = \frac{2,750}{A^{0.23}} \tag{29}$$

with a regression coefficient of $r^2 = 0.98$ and RMSE = 58.5. The shape of the curve, as expressed by the exponent, is similar to the values listed for Douglas-fir and Southern Pine glued-laminated beams (Rammer and Soltis 1994) and may be approximated as 1/5. The constant in Equation (29) represents shear strength corresponding to a shear area of 1 in^2 (16 cm^2). As noted earlier, the shear area of the ASTM block is 4 in^2 (64.5 cm^2). Thus, these equations can be rewritten in terms of the ASTM shear block strength rather than the shear strength corresponding to 1-in^2 shear area by including an adjustment factor of $4^{1/5}/1^{1/5} = 1.3$. Dividing the numerator by 2.6 (1.3×2) results in a value that falls within the observed ASTM shear block strengths. Thus, the following equation is recommended:

$$\tau = \frac{1.3\, C_{\mathrm{f}}\, \tau_{\mathrm{ASTM}}}{A^{1/5}} \tag{30}$$

This recommended equation relates beam shear strength to ASTM block shear strength, and it depends on the shear block stress concentration factor and the beam shear area.

Equation (30) is plotted for the Douglas-fir data in Figure 15. As the figure shows, this equation is a good approximation of the data from green specimens.

Comparison of Solid-Sawn and Glued-Laminated Beam Shear

Results from tests of solid-sawn beams were adjusted to 12 percent moisture content and 0.45 specific gravity to compare them with prior results from tests on glued-laminated beams. Experimental data were adjusted for specific gravity using the expressions developed in this report and those developed through the Western Wood Density Survey (Forest Products Laboratory 1965) for coast and interior west Douglas-fir (Table 5). Adjustments to 12 percent moisture content were made using the logarithmic moisture relationship developed by Wilson (1932) using three dry/green ratios. In addition to $S_{12}/S_{\mathrm{g}} = 1.61$, the published ASTM D2555 values for coast and interior west Douglas-fir, 1.25 and 1.38 (Table 10), were used. Finally, an MLE analysis was performed on the adjusted data to estimate the mean and standard deviation of the uncensored population. Figure 16 shows the estimated solid-sawn mean and glue-laminated mean Douglas-fir data from Rammer and Soltis (1994) along with the 95-percent confidence limits of the mean estimates. The proposed Equation (30) was plotted using the ASTM D2555 value adjusted to 12 percent moisture content (1,130 lb/in^2 (7.8 MPa)) for the glue-laminated data and the experimental value of 1,462 lb/in^2 (10.1 MPa) at 12 percent moisture content for the solid-sawn data.

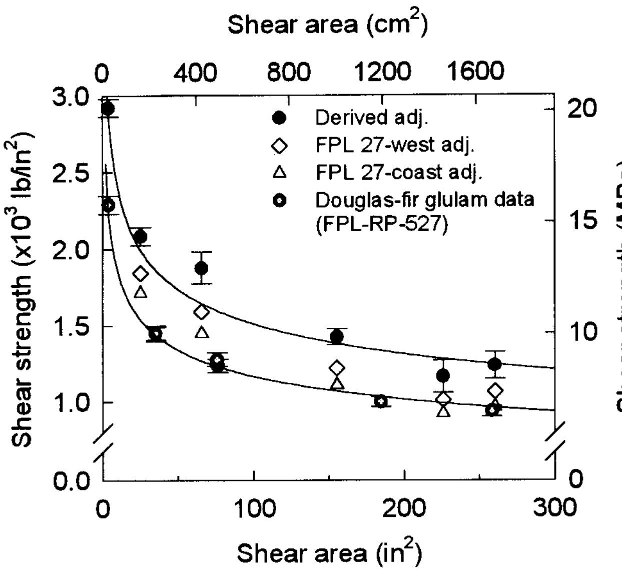

Figure 16—Comparison of shear moisture adjustments, previous glued-laminated shear strength results (Rammer and Soltis 1994), and proposed equations. Note: bottom curve was generated using ASTM shear block value of 1,130 lb/in^2 (7.8 MPa) and top curve using dry (adjusted to 12 percent moisture content) experimental shear block value of 1,462 lb/in^2 (10.1 MPa).

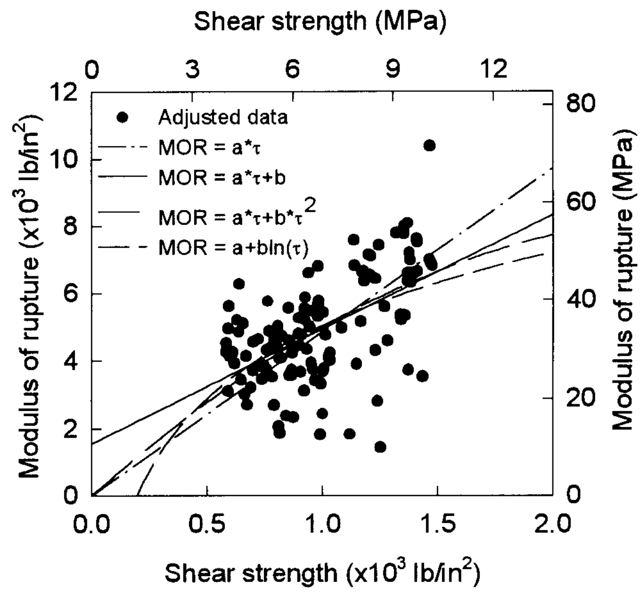

Figure 17—Modulus of rupture and shear strength of Douglas-fir at 24 percent moisture content and specific gravity of 0.45 (adjustments made assuming coast Douglas-fir relationships).

The figure shows similar trends in shear strength, but values for the solid-sawn material are greater than those for the glued-laminated beams for a dry/green ratio of 1.61. These higher values could indicate that the moisture adjustments based on shear blocks might not transfer to beam shear strength.

Shear to Bending Strength Relationship

While investigating the shear and compression properties of 2400f MSR lumber, Green and others (1994) investigated the relationship between shear strength and modulus of rupture. They plotted and regressed ASTM shear block strength against modulus of rupture and found a positive trend with a low coefficient of determination.

Similarly, Figure 17 shows some results of a regression analysis to determine whether a correlation exists between shear and bending strength of Douglas-fir beams. Several curves were regressed through various combinations of the shear and bending strength data to uncover any relationship. All bending and shear strength data, regardless of failure mode, were used to determine if any relationship existed. All strength data, except for the 2 by 4 specimens, were based on specimens matched by stress wave elastic modulus; data for the 2 by 4 specimens were end-matched. All data were adjusted to 24 percent moisture content and 0.45 specific gravity with Eq. (11) using ASTM dry/green ratios and Western Wood Density Survey (Forest Products Laboratory 1965) specific gravity relationships for modulus of rupture and shear strength. Modulus of rupture values were adjusted using the cross-sectional specific gravity and moisture content, whereas the beam shear strength values were adjusted using the local moisture content and specific gravity, as described earlier. The coefficient of determination (r^2) and RMSE values, as determined by Equations (23) and (24), of the regression analysis for all curves and combined sets are listed in Table 17. Overall, the r^2 values indicate a low correlation between beam shear strength and modulus of rupture.

Conclusions

In summary, 280 single-span third-point bending and five-point two-span beam shear tests were conducted on green solid-sawn Douglas-fir beams. Based on these experiments, a data set of both beam shear and ASTM block shear strength for unchecked, green Douglas-fir beams for a range of beam sizes from 2-by-4 to 4-by-14 cross-sections was developed. Our conclusions are as follow:

1. The five-point bending test procedure is recommended as a standard to measure beam shear. Consistent shear failures in an unchecked beam occurred between the loading point and middle support of the beam. The shear crack did not propagate to the end of the beam.

Table 17—Regressions relating shear strength to modulus of rupture[a]

	Coast DF		North DF		West DF	
Regressed equation	r^2	RMSE[b]	r^2	RMSE	r^2	RMSE
MOR = $a + b(\tau)$	0.31	1,333	0.27	1,357	0.28	1,352
MOR = $a + b(\tau) + c(\tau^2)$	0.36	1,279	0.32	1,315	0.34	1,303
MOR = $b(\tau) + c(\tau^2)$	0.28	1,359	0.25	1,379	0.26	1,376
MOR = $a(\tau^b)$	0.26	1,376	0.23	1,397	0.24	1,393
MOR = $ae^{b\tau}$	0.30	1,341	0.26	1,368	0.27	1,361
MOR = $a + b\ln(\tau)$	0.27	1,368	0.24	1,386	0.25	1,384

[a]DF is Douglas-fir.

2. Shear strength of green solid-sawn Douglas-fir beams varies with beam size. Larger beams have lower shear strength. Shear strength variation for various sizes of beams can be modeled with the following approximate equation, which is based on a relationship between beam shear and ASTM shear block strength, including a stress concentration factor for the re-entrant corner of the shear block:

$$\tau = \frac{1.3\, C_f \tau_{ASTM}}{A^{1/5}}$$

   This model is similar to that found previously for glued-laminated Douglas-fir and Southern Pine (Rammer and Soltis 1994).

3. Shear area parameter is preferred to beam volume or depth for modeling variation in shear strength based on a regression analysis.

4. The moisture adjustment based on dry/green shear block data may not be appropriate for beam shear. Further research is required.

5. There is little correlation between shear strength and modulus of rupture in matched solid-sawn beams.

Literature Cited

AF&PA. 1991. ANSI/NFPA NDS 1991 National design specification for wood construction. Washington, DC: American Forest & Paper Association formerly National Forest Products Association).

ASTM. 1995. Annual Book of Standards. Vol. 04.10.
D143-94–Standard methods of testing small clear specimens of timber.
D198-94–Static tests of timbers in structural sizes.
D245-93–Establishing structural grades and related allowable properties for visually graded lumber.
D1990-91–Establishing allowable properties for visually graded dimension lumber from in-grade tests of full-size specimens.
D2395-93–Standard test methods for specific gravity of wood and wood-base materials.
D2555-88–Establishing clear wood strength values.
D2915-94–Establishing allowable properties for grades of structural lumber.
D3043-87–Standard methods of testing structural panels in flexure.
D3737-93–Establishing stresses for structural glued laminated timber.
D4442-92–Standard test methods for direct moisture content measurement of wood and wood-base materials.
D4444-92–Standard test methods for use and calibration of hand-held moisture meters.
Philadelphia, PA: American Society for Testing and Materials.

Barrett, J.D. 1974. Effect of size on tension perpendicular-to-grain strength of Douglas-fir. Wood and Fiber Science. 6(2): 126–143.

Cramer, S.M.; Goodman, J.R.; Bodig, J.; Smith, F.W. 1984. Failure modeling of wood structural members. Structural Research 51. Fort Collins, CO: Civil Engineering Department, Colorado State University.

CSA. 1984. Engineering design in wood (working stress design). Ontario, Canada: Canadian Standards Association.

Ethington, R.L.; Galligan, W.L.; Montrey, H.M.; Freas, A.D. 1979. Evolution of allowable stresses in shear for lumber. Gen. Tech. Rep. FPL–GTR–23. Madison, WI: U.S. Department of Agriculture, Forest Service, Forest Products Laboratory.

Evans, J.W.; Green, D.W. 1987. Mechanical properties of visually graded lumber: Douglas-fir larch. Report on cooperative studies between the USDA Forest Service, Forest Products Laboratory; Northeastern Lumber Manufacturers Association, Inc.; Northern Hardwood and Pine Manufacturers Association; Southern Pine Inspection Bureau; West Coast Lumber Inspection Bureau; and Western Wood Products Association. Vol. 2.

Forest Products Laboratory. 1987. Wood Handbook: Wood as an engineering material. Agric. Handb. 72. (Rev.) Washington, DC: U.S. Department of Agriculture. 466 p.

Foschi, R.O.; Barrett, J.D. 1976. Longitudinal shear strength of Douglas-fir. Canadian Journal of Civil Engineering. 3: 198–208.

Foschi, R.O.; Barrett, J.D. 1977. Longitudinal shear in wood beams: A design method. Canadian Journal of Civil Engineering. 4: 363–370.

Green, D.W.; Kretschmann, D.E.; Fantozzi, J.A. 1994. Shear and compression perpendicular to grain property estimation for 2400f MSR lumber. Forest Products Journal. 44(11/12): 75–82.

Huggins, M.W.; Palmer, J.H.L.; Aplin, E.N. 1966. Evaluation of the effect of delamination. Engineering Journal. February, 32–41.

Keenan, F.J. 1974. Shear strength of wood beams. Forest Products Journal. 24(9): 63–70.

Keenan, F.J.; Kryla, J.; Kyokong, B. 1985. Shear strength of spruce glued-laminated timber beams. Canadian Journal of Civil Engineering. 12: 661–672.

Kvålseth, T.O. 1985. Cautionary note about r^2. The American Statistician. 39(4). Part 1.

Lawless, J.F. 1982. Statistical models and methods for lifetime data. New York: John Wiley and Sons. 580 p.

Leicester, R.H.; Breitinger, H.O. 1992. Measurement of shear strength. In: Proceedings, 1992 IUFRO S5.02 Timber Engineering Conference, Nacy, France. p. 287–299.
Longworth, J. 1977. Longitudinal shear strength of timber beams. Forest Products Journal. 27(8): 19–23.

Mood, A.M.; Graybill, F.A.; Boes, D.C. 1974. Introduction to the theory of statistics. New York: McGraw–Hill Book Co. 564 p.

Nelson, W. 1982. Applied life data analysis. New York: John Wiley and Sons: 522–539.

Newlin, J.W; Heck, G.E.; March, H.W. 1934. New method of calculating longitudinal shear in checked wooden beams. Transactions ASME: 56(10): 739–744.

Quaile, A.T.; Keenan, F.J. 1978. Shear strength of small composite wood beams. Wood Science. 11(1): 1–9.

Radcliffe, B.M.; Suddarth, S.K. 1955. The notched beam shear test for wood. Forest Products Journal. 5(2): 131–135.

Rammer, D.R.; Soltis, L.A. 1994. Experimental shear strength of glued-laminated beams. Res. Rep. FPL–RP–527. Madison, WI: U.S. Department of Agriculture, Forest Service, Forest Products Laboratory.

Ross, R.J.; Pellerin, R.F. 1991. NDE of green material with stress waves: Preliminary results using dimensional lumber. Forest Products Journal. 41(6): 57–59.

Ross, R.J.; Pellerin, R.F. 1994. Nondestructive testing for assessing wood members in structures: A review. Gen. Tech. Rep. FPL–GTR–70. Madison, WI: U.S. Department of Agriculture, Forest Service, Forest Products Laboratory.

SAS Institute Inc. 1988. SAS/STAT User Guide Release. 6.03 Edition. Cray, NC. 1,028 p.

Weibull, W. 1939. A statistical theory of the strength of materials. In Proceedings, Swedish Royal Institute of Engineering Research No. 151, Stockholm, Sweden.

Western Wood Density Survey. 1965. Res. Rep. FPL 27. Madison, WI: U.S. Department of Agriculture, Forest Service, Forest Products Laboratory.

Wilson, T.R.C. 1932. Strength–moisture relations for wood. Tech. Bull. 282. Madison, WI: U.S. Department of Agriculture, Forest Service, Forest Products Laboratory.

Yeh, B.J. 1993. Shear strength of Douglas-fir structural glued-laminated timber. AWS Rep. T93-2. Tacoma, WA: American Wood Systems–American Plywood Association. p. 13.

Appendix A—Details of Experimental Deflection Procedures

This appendix contains information about the measurement of modulus of elasticity during bending tests conducted on beams larger than 2 by 4 beams. Figure A1 illustrates the testing configuration and parameters, and Table A1 gives specific information about the parameter for each test.

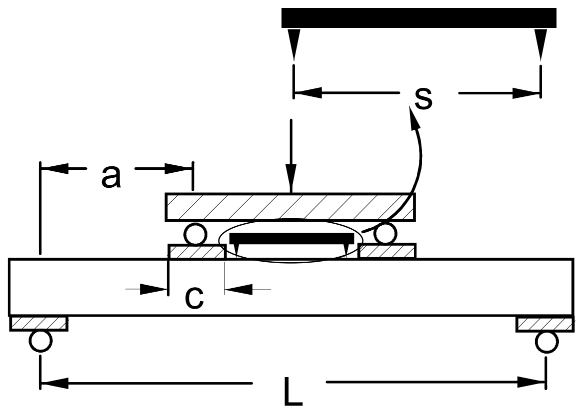

Figure A1–Bending test configuration with middle ordinate deflectometer.

Table A1—Parameters of deflection measurement for each size of beams[a]

Beam size	Span length L (in.)	Shear span a (in.)	Measurement span s (in.)	Plate size c (in.)	LVDT throw[b] (in.)
2 by 10	$138^3/_4$	$46^1/_4$	36	3	0.2
4 by 8	112	$37^1/_3$	30	2	0.2
4 by 12	$176^1/_4$	$59^1/_4$	48	3	1.0
4 by 14	$206^1/_4$	$68^3/_4$	60	4	1.0

[a]1 in. = 25.4 mm.
[b]Maximum recordable deflection for LVDT.

Appendix B—Five-Point Shear Results for Solid-Sawn Douglas-fir

Appendix B contains tables with experimental results from the five-point shear tests. Results include dimensions, mechanical properties (stiffness and strength), and a description of the type of failure for green Douglas-fir lumber. Note that the modulus of elasticity (MOE) values were determined by a stress wave technique at the time of material delivery and are not at the same moisture content published in the tables. Electric moisture meter readings were taken near the failure crack, and section values are cross-section averages by ASTM procedure.

Table B1—Shear test results for 4 by 14 beams[a]

					Moisture content							
Beam no.	Depth (in.)	Width (in.)	Length (in.)	Weight (lb)	Meter (%)	Sect. (%)	Specific gravity	MOE ($\times 10^6$ lb/in^2)	Time to failure (min:s)	Failure load (lb)	Shear (lb/in^2)	Failure type[b]
301	13.66	3.75	168.8	162	24.0	23.1	0.41	1.68	19:33	57,600	580	Shear
302	13.78	3.78	168.3	181	21.5	24.1	0.45	1.44	8:39	73,400	726	Shear
304	13.91	3.97	169.4	189	24.5	25.8	0.47	1.48	10:24	70,600	660	Shear
312	13.94	3.88	170.0	207	25.5	26.8	0.40	1.31	20:01	77,200	737	Shear
315	13.78	3.75	168.6	191	23.5	26.3	0.41	1.10	8:11	76,600	764	Shear
317	13.75	3.75	169.3	193	22.5	26.4	0.47	1.21	15:26	89,000	890	Shear
320	13.84	3.75	169.5	181	24.0	24.6	0.45	1.85	21:00	80,000	795	Comp.
322	13.69	3.66	169.0	176	23.5	26.6	0.42	1.60	19:45	66,600	686	Shear
328	13.53	3.75	169.3	169	27.0	26.7	0.43	1.56	12:10	67,500	686	Shear
329	13.66	3.81	169.5	160	24.0	26.3	0.37	1.23	18:42	69,200	685	Shear
331	13.78	3.75	169.0	172	23.5	25.1	0.39	0.96	7:32	91,200	910	Shear
335	13.81	3.81	169.3	196	28.0	28.6	0.45	1.30	15:45	68,200	668	Shear
339	13.84	3.78	168.9	196	25.5	29.6	0.43	2.18	8:50	64,000	630	Shear
342	13.78	3.59	169.4	179	24.0	24.7	0.45	1.28	15:45	71,000	739	Shear
349	13.78	3.81	169.0	179	26.0	26.7	0.44	1.40	14:47	73,800	724	Shear
350	13.72	3.72	168.9	173	21.0	25.7	0.42	1.34	9:05	86,600	875	Shear
352	13.88	3.75	169.4	188	22.7	31.6	0.40	1.01	13:40	75,600	749	MOR
353	13.75	3.78	169.6	184	20.0	21.8	0.44	1.54	6:25	64,300	638	Shear
354	13.66	3.75	169.6	194	25.0	25.3	0.50	1.64	12:40	73,700	742	Shear
360	13.66	3.78	169.4	159	20.0	22.8	0.34	1.15	16:31	90,800	907	MOR

[a]1 in. = 25.4 mm; 1 lb = 0.454 kg; 1 lb/in^2 = 6.894 kPa.

[b]Comp. is compression; MOR, modulus of rupture.

Table B2—Shear test results for 4 by 12 beams

Beam no.	Depth (in.)	Width (in.)	Length (in.)	Weight (lb)	Moisture content Meter (%)	Moisture content Sect. (%)	Specific gravity	MOE ($\times 10^6$ lb/in²)	Time to failure (min:s)	Failure load (lb)	Shear (lb/in²)	Failure type[b]
161	11.88	3.84	144.4	116	21	20.5	0.39	1.13	7:30	53,400	603	Shear
162	11.88	3.84	144.9	126	23	21.5	0.44	1.27	14:24	50,900	575	Shear
166	11.75	3.84	144.9	152	24	21.4	0.47	1.31	17:45	85,000	970	MOR
170	11.94	3.94	144.4	119.5	18	21.8	0.38	1.00	14:31	68,500	751	Shear
175	11.66	3.69	145.0	143	24.5	28.2	0.50	1.61	12:19	63,400	761	Shear
177	11.81	3.88	145.0	149	22	19.6	0.46	1.51	7:07	66,000	743	Shear
179	11.94	3.94	144.5	145	26	28.7	0.39	1.17	13:33	67,200	737	Shear
181	11.84	3.75	144.5	137	27	28.4	0.45	1.63	17:35	69,200	803	Shear
184	11.91	3.75	144.4	133	25.5	24.6	0.49	1.46	16:10	59,900	692	Shear
188	11.91	3.94	144.5	153	25	25.5	0.54	1.84	19:06	66,500	731	Shear
191	11.81	3.84	144.5	201	30	93.4	0.53	2.24	17:52	63,200	718	Shear
192	11.72	3.88	145.0	171	29	43.9	0.49	1.22	11:32	57,000	647	Shear
203	11.72	3.88	144.4	126	24.5	21.6	0.38	1.34	12:16	70,400	799	Shear
207	11.94	3.78	144.6	134	27.5	23.7	0.41	1.41	25:00	82,400	941	MOR
210	12.10	3.75	144.5	157	26.5	31.1	0.46	1.82	22:23	57,500	654	Shear
211	11.79	3.88	144.6	122	25.5	24.1	0.40	1.37	6:10	45,200	510	Shear
213	11.88	3.84	144.5	137	23.5	20.1	0.53	1.69	20:40	78,600	888	Shear
216	12.00	4.00	144.5	146	24	20.8	0.49	1.41	13:40	62,400	670	MOR
217	11.81	3.84	144.5	139	22	21.3	0.50	1.91	18:45	96,000	1,090	Shear
219	11.88	3.78	144.4	134	22.5	21.5	0.47	1.59	13:34	57,800	664	Shear

Table B3—Shear test results for 4 by 8 beams

Beam no.	Depth (in.)	Width (in.)	Length (in.)	Weight (lb)	Moisture content: Meter (%)	Moisture content: Sect. (%)	Specific gravity	MOE ($\times 10^6$ lb/in^2)	Time to failure (min:s)	Failure load (lb)	Shear (lb/in^2)	Failure type[b]
3	7.94	3.91	96.5	74	23	21.4	0.57	2.37	10:57	68,000	1,131	Shear
5	8.00	3.88	96.5	62.5	22.5	24.2	0.48	1.25	12:15	57,600	958	MOR
7	8.00	3.88	96.1	56.5	23.5	27.1	0.39	1.55	13:56	51,500	857	Shear
10	7.84	3.75	96.3	69	28.5	33.5	0.55	1.60	10:56	57,000	999	Shear
15	7.97	3.84	96.4	54	24	27.4	0.41	1.26	15:36	48,200	811	Shear
20	7.78	4.19	96.4	61	21.5	22.3	0.43	1.29	9:39	49,400	782	Shear
25	7.88	3.94	96.5	61	26	27.1	0.42	1.05	13:04	51,800	861	Shear
27	7.94	3.88	96.6	67	25	33.4	0.47	1.47	15:34	56,600	949	Shear
28	7.91	3.88	96.1	56	24.5	28.9	0.40	1.39	13:44	46,500	783	Shear
33	7.94	3.88	96.3	64	25	27.8	0.50	1.60	18:09	63,600	1,066	MOR
36	8.00	3.81	96.5	49	24	26.2	0.35	1.14	14:21	42,100	712	Shear
37	7.97	3.84	96.6	60	25.5	37.2	0.42	1.22	18:45	40,800	687	MOR
38	7.94	3.97	96.6	70	25	29.9	0.48	1.80	11:16	58,200	953	Shear
39	7.94	4.00	96.5	71	26	33.1	0.52	1.82	15:00	59,800	971	Shear
40	7.94	3.81	96.4	53	26	30.7	0.36	1.32	13:05	42,400	722	MOR
42	7.88	3.91	96.5	59	26	27.5	0.43	1.55	14:39	55,000	922	Shear
43	7.88	3.88	96.5	60	25	28.0	0.44	1.49	10:40	50,200	848	Shear
47	8.03	3.88	96.5	71	26	41.2	0.48	1.65	11:06	53,400	885	MOR
48	7.88	3.97	96.5	62	27.5	33.2	0.43	0.94	12:00	44,600	736	MOR
50	8.00	3.78	96.5	56	26	33.4	0.37	1.02	15:28	44,600	760	Shear
53	8.06	3.88	96.5	57	27	32.9	0.43	1.16	15:52	47,100	777	Shear
54	7.97	3.94	96.5	64	25.5	41.5	0.43	1.30	13:24	43,800	720	MOR
61	7.81	3.84	96.6	70	26	30.2	0.50	1.93	13:43	58,200	999	Shear
67	8.00	3.84	96.5	59	25	27.8	0.41	1.23	13:16	51,100	857	MOR
70	7.81	3.97	69.6	70	25	27.9	0.49	2.10	10:02	51,600	858	Shear
76	7.97	3.88	96.5	54	19.5	25.7	0.43	0.76	15:52	47,100	786	Shear
77	8.03	4.00	96.6	65	27	32.7	0.46	1.35	9:36	57,400	921	MOR
80	8.00	3.94	96.5	58	25	28.3	0.40	1.21	12:53	41,000	671	Shear
81	7.88	3.97	96.6	70	23.5	28.3	0.57	2.17	10:29	56,400	930	Shear
87	7.88	3.88	96.6	64	26	36.3	0.42	1.45	10:16	45,700	772	Shear
89	8.00	3.84	96.5	61	24	27.8	0.43	1.10	8:38	44,000	738	Shear
91	8.06	3.88	96.6	57	22.5	24.3	0.41	1.51	11:04	49,600	819	Shear
92	8.00	3.84	96.6	70	25.5	29.9	0.51	2.31	12:16	58,200	976	Shear
94	7.97	3.88	96.5	75	25.5	29.6	0.51	1.74	11:30	66,200	1,105	Shear
100	8.06	3.84	96.6	58	24.5	22.8	0.43	1.52	12:17	55,400	922	Shear
102	8.19	3.84	96.5	62.5	24.5	29.4	0.42	1.34	15:12	59,300	972	Shear
106	7.94	3.88	96.5	53	24	26.5	0.39	1.41	12:30	50,600	848	Shear
107	7.84	3.88	96.5	52	22	22.4	0.39	1.68	13:27	51,100	867	Shear
113	7.94	3.78	96.5	53	20.5	23.6	0.40	1.36	8:30	40,800	701	Shear
118	8.34	3.81	96.5	56	20.5	23.9	0.42	1.17	11:02	43,500	705	MOR

Table B4—Shear test results for 2 by 10 beams

					Moisture content							
Beam no.	Depth (in.)	Width (in.)	Length (in.)	Weight (lb)	Meter (%)	Sect. (%)	Specific gravity	MOE ($\times 10^6$ lb/in^2)	Time to failure (min:s)	Failure load (lb)	Shear (lb/in^2)	Failure type[b]
562	9.03	1.33	144.63	33	17	15.6	0.47	1.59	10:26	22,803	981	MOR
564	9.14	1.34	144.50	31	16	16.9	0.42	0.95	6:45	22,241	938	MOR
568	9.27	1.42	144.25	38	21	21.3	0.45	1.60	5:48	32,153	1,258	Shear
572	9.28	1.42	144.50	39.5	20	20.6	0.49	2.22	13:47	27,490	1,076	Shear
576	9.12	1.32	144.50	38	23	19.7	0.51	1.97	—	26,221	1,119	Comp.
581	9.27	1.43	144.25	36	22	19.3	0.44	1.25	5:09	30,688	1,197	Shear
585	9.26	1.44	144.50	37	30	34.3	0.41	1.45	6:44	21,362	829	MOR
589	9.36	1.46	144.25	45	30	25.1	0.47	1.43	10:30	24,090	910	MOR
591	9.26	1.32	144.25	34	24	33.5	0.38	1.30	—	21,826	919	Shear
594	9.30	1.35	146.25	43	30	35.9	0.46	1.22	8:20	22,363	922	MOR
595	9.29	1.34	144.38	33.5	22	27.2	0.41	0.90	4:48	24,218	1,002	Shear
596	9.35	1.44	145.00	38	27	31.7	0.41	1.14	7:36	25,439	975	MOR
600	9.36	1.43	145.00	41	26	24.4	0.50	1.23	6:20	20,093	776	Shear
602	9.36	1.50	144.63	42	24	32.6	0.43	1.26	4:35	23,193	850	MOR
604	9.33	1.39	144.44	39	25	26.7	0.48	1.70	4:56	19,824	791	Shear
609	9.35	1.44	144.50	38	22	22.4	0.42	1.39	—	19,580	749	Comp.
610	9.40	1.41	144.38	37	30	48.6	0.38	1.15	8:15	21,826	850	MOR
614	9.39	1.44	146.25	41.5	27	37.6	0.43	1.72	7:58	24,561	937	Shear
623	9.29	1.35	144.50	33.5	25	28.1	0.38	1.04	10:06	18,335	757	MOR
624	9.37	1.39	144.44	35	30	31.9	0.36	0.96	8:09	17,114	1,039	MOR
625	9.29	1.41	144.50	32.5	25	21.3	0.38	1.21	7:15	15,259	924	Shear
626	9.42	1.47	144.13	42	26	29.2	0.47	1.66	13:37	29,101	1,081	Shear
627	9.40	1.44	144.50	38.5	30	32.3	0.44	1.19	12:00	23,779	905	MOR
631	9.38	1.46	144.25	38.5	26	26.3	0.42	1.41	7:08	27,589	1,038	MOR
634	9.43	1.48	144.25	37.5	27	50.0	0.39	1.13	4:35	14,429	535	MOR
635	9.40	1.46	144.13	35	25	33.9	0.39	1.37	13:03	19,409	731	Comp.
644	9.40	1.45	144.13	31	24	25.6	0.32	0.84	8:45	20,435	775	MOR
645	9.32	1.38	144.13	31	24	27.3	0.36	1.05	5:33	19,214	773	MOR
646	9.36	1.45	144.13	33.5	23	22.1	0.37	1.12	10:3	22,144	841	MOR
648	9.42	1.48	144.13	39	27	35.9	0.40	1.36	10:4	26,397	976	MOR
649	9.42	1.43	144.13	39	24	25.0	0.44	1.75	17:15	24,097	924	Comp.
650	9.37	1.46	144.00	38.5	23	20.7	0.44	1.77	8:30	24,512	927	MOR
651	9.41	1.48	144.13	39	28	35.6	0.42	1.54	10:04	23,999	890	MOR
652	9.22	1.33	144.00	31	24	28.1	0.36	1.01	5:15	24,780	1,044	MOR
658	9.40	1.41	144.13	32.5	20	20.4	0.36	1.27	9:00	25,317	984	Shear
664	9.33	1.33	144.13	31	25	24.8	0.39	1.33	8:23	19,482	813	MOR
668	9.30	1.43	144.13	31	19	20.7	0.39	0.99	5:35	19,629	761	MOR
678	9.35	1.44	144.13	34	23	23.4	0.41	1.50	8:15	24,292	928	MOR
679	9.20	1.42	144.13	32	16	17.0	0.38	1.38	10:34	32,568	1,282	MOR
680	9.26	1.48	144.00	34.5	21	18.8	0.40	1.16	4:59	22,363	841	MOR

Table B5—Shear test results for 2 by 4 beams

Beam no.	Depth (in.)	Width (in.)	Length (in.)	Weight (lb)	Moisture content: Meter (%)	Moisture content: Sect. (%)	Specific gravity	MOE ($\times 10^6$ lb/in^2)	Time to failure (min:s)	Failure load (lb)	Shear (lb/in^2)	Failure type[b]
363	3.43	1.43	51.3	5.2	20	21.1	0.47	2.06	9:58	12,305	1,293	Shear
376	3.44	1.46	51.3	4.6	22	23.8	0.40	1.15	5:37	13,110	1,347	Shear
377	3.42	1.42	51.3	5.0	20	25.2	0.46	1.80	13:59	12,744	1,352	Shear
381	3.41	1.44	51.3	4.7	20	20.3	0.41	1.74	10:47	13,452	1,409	Shear
386	3.45	1.43	51.3	5.0	22	23.8	0.45	1.78	12:03	13,648	1,429	Shear
387	3.43	1.44	51.3	5.1	24	25.8	0.44	1.08	6:23	12,354	1,285	Shear
388	3.39	1.43	51.3	5.1	18	19.9	0.45	1.66	17:08	14,233	1,511	Shear
395	3.41	1.44	51.3	5.4	24	24.2	0.46	2.16	9:51	12,964	1,365	Shear
396	3.42	1.45	51.3	4.3	18	22.1	0.40	1.27	7:17	11,060	1,151	MOR
398	3.44	1.46	51.3	4.9	25	30.6	0.39	1.50	10:20	11,987	1,232	MOR
399	3.41	1.44	51.3	4.0	20	22.4	0.37	1.61	11:31	10,830	1,141	Shear
402	3.41	1.44	51.3	4.5	22	23.2	0.40	1.47	16:22	11,841	1,242	Shear
404	3.40	1.42	51.3	6.4	19	22.4	0.58	2.94	7:15	17,090	1,818	Shear
405	3.45	1.43	51.3	4.7	22	25.3	0.40	1.33	9:24	11,377	1,188	MOR
408	3.43	1.44	51.3	5.1	23	23.1	0.45	1.72	13:03	13,572	1,412	Shear
410	3.45	1.44	51.3	4.6	22	25.3	0.40	1.69	11:39	10,693	1,110	MOR
411	3.46	1.44	51.3	4.9	24	27.9	0.41	1.59	8:37	10,645	1,105	Shear
413	3.44	1.44	51.3	5.9	23	24.9	0.49	2.41	3:41	14,331	1,491	Shear
415	3.46	1.44	51.3	4.8	21	23.6	0.33	1.25	10:09	9,863	1,022	MOR
417	3.46	1.46	51.3	6.3	23	27.7	0.53	2.12	7:27	15,576	1,585	Shear
423	3.43	1.48	51.3	4.2	20	23.5	0.39	1.36	8:55	10,278	1,046	MOR
424	3.42	1.44	51.3	5.0	21	24.1	0.42	1.62	13:26	13,574	1,424	Comp.
429	3.43	1.42	51.3	5.2	19	23.2	0.46	2.11	7:04	14,551	1,535	Shear
433	3.45	1.43	51.3	5.4	22	21.7	0.47	2.02	9:22	13,477	1,406	Shear
435	3.45	1.43	51.3	4.4	24	25.7	0.38	1.11	11:21	12,378	1,293	MOR
438	3.44	1.44	51.3	4.9	24	35.9	0.39	1.17	11:04	12,451	1,296	MOR
443	3.44	1.45	51.3	4.7	21	23.6	0.40	1.43	11:06	12,476	1,290	Comp.
447	3.45	1.44	51.3	5.0	20	22.7	0.44	1.45	9:28	15,503	1,603	Shear
450	3.40	1.41	51.3	4.8	12	14.9	0.47	1.91	10:17	14,697	1,579	Comp.
451	3.44	1.44	51.3	5.4	22	22.3	0.47	1.77	8:57	13,818	1,438	Shear
453	3.39	1.44	51.3	4.5	19.5	19.4	0.44	1.42	13:11	13,989	1,478	Comp.
456	3.42	1.47	51.3	4.6	20	24.1	0.40	1.51	9:23	12,036	1,234	Shear
467	3.45	1.45	51.3	5.2	20	22.2	0.46	1.85	9:38	14,331	1,481	Shear
468	3.40	1.42	51.3	5.2	17	18.7	0.48	1.94	15:31	15,161	1,616	Shear
470	3.43	1.43	51.3	4.5	20	22.2	0.40	1.46	12:32	11,865	1,247	MOR
471	3.42	1.43	51.3	5.3	19	20.9	0.50	2.28	12:15	15,234	1,607	MOR
472	3.38	1.42	51.3	5.5	17	17.9	0.51	2.31	14:27	16,260	1,749	Shear
473	3.41	1.43	51.3	4.5	21	22.9	0.40	1.56	14:08	11,914	1,265	MOR
474	3.44	1.44	51.3	5.4	18.5	22.1	0.46	1.64	12:56	13,501	1,400	Shear
475	3.43	1.43	51.3	4.4	19	20.4	0.39	1.19	10:05	13,013	1,373	MOR

Appendix C—Third-Point Bending Results for Solid-Sawn Douglas-fir

Appendix C contains tables with experimental results from the third-point bending tests. The data include dimensions, mechanical properties (stiffness and strength), and description of the type of failure for green Douglas-fir lumber. Note that the modulus of elasticity (MOE) values were determined during experimental testing from the load versus deflection curve.

Table C1—Bending test results for 4 by 14 beams[a]

Beam no.	Depth (in.)	Width (in.)	Length (in.)	Weight (lb)	MC (%)	Specific gravity	MOE ($\times 10^6$ lb/in^2)	Time to failure (min:s)	Failure load (lb)	MOR (lb/in^2)	Comment
261	13.81	3.88	217.00	219	23.5	0.42	1.25	12:40	17,600	4,910	Cross-grain tension failure
262	13.75	3.75	217.06	236	24.5	0.46	1.35	13:12	17,100	4,975	Cross-grain failure
264	13.81	3.91	215.75	246	27.3	0.48	1.66	9:52	19,000	5,258	Cross-grain failure
266	13.84	3.81	217.81	250	25.0	0.46	1.75	7:49	14,350	4,051	Tension failure at midspan knot
271	13.94	4.00	217.00	276	24.5	0.50	1.61	7:25	14,090	3,740	Cross-grain tension failure
272	13.69	3.78	216.50	212	18.2	0.45	2.22	6:20	17,890	5,209	Splintering tension
275	13.69	3.66	216.50	257	20.8	0.53	2.51	13:10	24,800	7,467	Cross-grain tension failure
276	13.81	3.75	216.25	216	21.6	0.42	1.38	9:00	8,193	2,362	Tension failure at 3-in. diameter midspan knot
278	13.75	3.75	217.00	226	20.0	0.49	1.92	8:45	19,560	5,690	Tension failure at midspan knot
279	13.84	3.94	216.25	236	21.4	0.43	1.82	10:00	19,600	5,357	Cross-grain failure near knot
280	13.94	3.78	216.75	244	23.0	0.44	1.11	9:03	7,900	2,218	Tension failure at knot
281	13.81	3.75	216.75	223	21.5	0.45	1.71	9:36	15,670	4,517	Splintering tension failure at spike knot
284	13.56	3.75	217.75	205	18.3	0.40	0.68	16:29	5,200	1,555	Splintering tension at knot
285	13.91	3.81	217.00	220	26.3	0.40	0.65	7:30	2,800	783	Tension failure at 5-in. diameter knot
287	13.75	3.75	216.25	223	19.3	0.45	1.19	7:32	7,750	2,255	Slope-of-grain failure at 2-in. diameter knot
288	13.72	3.78	216.50	238	22.5	0.45	1.27	14:22	12,700	3,681	Cross-grain/splintering tension failure
289	13.75	3.75	216.50	244	23.6	0.47	1.52	9:12	14,900	4,335	Cross-grain failure near knot
290	13.75	3.75	216.38	198	18.7	0.42	1.46	9:15	8,000	2,327	Tension failure at 6- by 2-in. elliptical knot
293	13.91	3.78	216.50	268	22.5	0.53	1.96	13:52	18,900	5,331	Splintering tension at knot
296	13.75	3.88	215.25	224	20.3	0.44	1.98	13:00	18,000	5,067	Cross-grain failure at knot

[a]MC is moisture content.

Table C2—Bending test results for 4 by 12 beams

Beam no.	Depth (in.)	Width (in.)	Length (in.)	Weight (lb)	MC (%)	Specific gravity	MOE ($\times 10^6$ lb/in^2)	Time to failure (min:s)	Failure load (lb)	MOR (lb/in^2)	Comment
222	11.69	3.75	192.25	166	21.6	0.44	2.30	9:55	15,100	5,240	Splintering tension
224	11.81	3.75	192.50	159	21.3	0.39	1.00	6:25	6,200	2,106	Tension failure at knot
225	11.66	3.84	192.25	169	24.5	0.43	1.80	18:35	17,200	5,854	Compression
227	11.63	3.75	193.13	152	25.4	0.39	1.89	6:15	7,000	2,455	Slope-of-grain failure at knot
232	11.69	3.84	192.25	172	24.8	0.40	1.58	6:45	9,700	3,284	Tension failure at knot
234	11.69	3.75	193.13	220	83.1	0.45	2.52	15:10	16,200	5,621	Simple tension
240	11.81	3.72	192.25	169	28.5	0.41	1.06	13:25	11,700	4,008	Simple tension failure
242	11.69	3.72	193.00	149	28.1	0.39	1.26	8:30	6,900	2,414	Simple tension at knot
243	11.59	3.78	192.25	155	28.8	0.43	1.79	8:35	10,000	3,497	Cross-grain failure at knot
245	11.75	3.91	193.00	187	51.7	0.41	1.60	7:00	6,900	2,274	Slope-of-grain failure at knot
246	11.81	3.91	192.25	194	31.7	0.44	2.02	10:30	14,100	4,598	Cross-grain / simple tension failure at knot
247	11.75	3.88	192.25	167	38.8	0.38	1.22	10:34	9,800	3,256	Slope-of-grain failure at 3-in. knot
248	11.69	3.88	192.38	180	27.6	0.45	1.79	12:30	10,200	3,425	Tension failure at spike knot
249	11.81	3.84	192.25	175	29.8	0.45	1.74	15:46	11,300	3,745	Slope-of-grain failure at encased knot
250	11.81	3.81	193.00	189	60.0	0.40	1.30	6:10	6,500	2,172	Cross-grain failure
251	12.19	3.88	193.13	166	32.1	0.36	1.11	9:10	8,100	2,501	Slope-of-grain failure
254	11.84	3.78	192.25	178	24.2	0.45	1.38	8:35	14,200	4,759	Brash tension failure at knot
257	11.63	3.81	192.00	158	23.4	0.43	1.88	10:09	12,200	4,209	Slope-of-grain failure
259	11.63	3.78	193.00	168	24.3	0.40	1.53	8:39	9,200	3,200	Splintering tension
260	11.69	3.75	192.50	143	19.5	0.38	1.25	9:07	10,500	3,644	Slope-of-grain failure

Table C3—Bending test results for 4 by 8 beams

Beam no.	Depth (in.)	Width (in.)	Length (in.)	Weight (lb)	MC (%)	Specific gravity	MOE ($\times 10^6$ lb/in^2)	Time to failure (min:s)	Failure load (lb)	MOR (lb/in^2)	Comment
121	7.94	3.81	120.50	64	21.4	0.38	1.33	5.25	7,886	3,677	Tension failure at knot
123	8.00	3.78	120.50	67	28.6	0.39	1.25	7.06	7,642	3,537	Splintering tension failure
124	8.09	3.91	120.19	69	28.4	0.40	1.62	12.11	9,082	3,975	Brash tension failure near knot
126	7.98	3.84	120.50	69	25.0	0.39	1.44	7.28	9,838	4,503	Slope-of-grain failure
127	7.91	4.10	120.50	93	53.9	0.45	1.53	7.06	9,302	4,061	Brash tension failure at knot
129	7.87	3.88	120.44	92	36.9	0.52	1.80	12.24	13,354	6,220	Tension failure at knot
130	8.17	3.82	120.56	99	40.5	0.52	2.03	13.18	13,818	6,062	Compression failure near top knot
132	8.02	3.80	120.50	82	27.4	0.47	2.07	12.2	8,618	3,949	Tensile failure at knot
133	7.89	3.92	120.50	91.5	37.7	0.51	1.99	16.26	15,015	6,896	Compression failure at midspan
134	8.06	3.88	120.44	85.5	34.8	0.45	1.91	8.47	10,986	4,875	Tension failure at lower knot
135	8.14	3.85	120.50	73.5	32.3	0.41	1.36	8.27	10,742	4,715	Splintering tension near spike knot
138	7.88	3.84	120.56	78	26.7	0.47	1.98	8.34	11,963	5,620	Slope-of-grain failure
139	7.79	3.78	120.50	63	28.9	0.38	0.49	12.15	4,663	2,278	Splintering tension at existing cracks
144	7.84	3.74	121.38	73	25.3	0.42	1.81	8.56	9,937	4,843	Splintering tension near knot
147	7.87	3.77	120.63	77.5	37.2	0.43	1.94	6.11	9,565	4,585	Slope of grain failure
149	8.02	3.89	120.56	69.5	28.2	0.40	1.44	6.22	7,593	3,400	Cross/slope-of-grain failure
151	7.90	3.99	120.50	68	26.3	0.40	2.22	10.3	12,354	5,555	Simple tension near knot
152	7.80	4.06	120.50	87	29.6	0.48	1.84	12.43	12,964	5,886	Splintering tension failure in knotty region
155	7.94	3.97	120.50	69	26.6	0.38	1.06	5.48	6,372	2,851	Splintering tension at midspan
160	7.82	3.80	120.50	65.5	25.1	0.39	1.19	6.45	4,810	2,318	Shear failure

Table C4—Bending test results for 2 by 10 beams

Beam no.	Depth (in.)	Width (in.)	Length (in.)	Weight (lb)	MC (%)	Specific gravity	MOE ($\times 10^6$ lb/in^2)	Time to failure (min:s)	Failure load (lb)	MOR (lb/in^2)	Comment
484	9.33	1.47	168.25	43	22.6	0.41	1.45	4.58	3,062	3,326	Splintering tension at knot
491	9.38	1.47	168.25	39	24.3	0.36	0.80	5.35	2,358	2,532	Brash tension failure near knot
492	9.40	1.49	168.25	42	29.4	0.35	2.46	8.35	3,592	3,781	Slope-of-grain failure
493	9.40	1.45	168.38	42.5	25.5	0.38	1.22	7.23	3,779	4,080	Splintering tension failure
494	9.40	1.47	168.25	48	30.6	0.39	1.33	8.11	2,780	2,978	Slope-of-grain failure caused by grain deviation near knot
496	9.40	1.46	168.25	46	36.3	0.37	1.29	8.03	3,062	3,289	Slope-of-grain failure caused by grain deviation near knot
509	9.29	1.48	168.25	42	20.6	0.39	1.22	6.35	2,796	3,037	Slope-of-grain failure near knots
510	9.39	1.49	168.25		23.2	0.36	9.90	9.19	3,423	3,606	Cross-grain failure
512	9.25	1.31	168.25	48	20.8	0.48	1.55	5.00	2,192	2,708	Slope-of-grain at knot
514	9.35	1.46	168.25	47	22.4	0.45	1.44	6.44	2,393	2,603	Tension failure at knot
515	9.31	1.45	168.25	36	100.0	0.37	1.27	9.09	3,462	3,829	Brash tension failure
520	9.26	1.46	168.25	42	20.1	0.40	1.70	7.39	3,506	3,895	Tension failure at knot
521	9.39	1.47	168.25	47	23.5	0.42	1.06	4.28	2,583	2,770	Brash tension failure near knot
525	9.36	1.44	168.25	38	23.4	0.35	0.81	5.34	1,914	2,099	Tension failure at spike knot
534	9.35	1.49	168.25	45	29.2	0.40	0.83	6.06	2,564	2,726	Abrupt tension failure near knot (cross grain)
535	9.30	1.46	168.25	45	22.0	0.42	0.81	8.20	2,505	2,749	Tension failure near knot
541	9.44	1.47	168.25	45	30.5	0.37	1.36	12.25	4,839	5,119	Splintering tension caused by inelastic buckling
548	9.38	1.46	168.25	42	22.5	0.36	1.43	9.10	3,926	4,243	Brash tension failure at knot
556	9.31	1.45	168.25	54	20.7	0.52	0.48	5.19	5,161	5,678	Slope-of-grain failure
558	9.33	1.47	168.25	40	21.4	0.38	0.94	6.26	2,324	2,512	Tension failure near knot

Table C5—Bending test results for 2 by 4 beams

Beam no.	Depth (in.)	Width (in.)	Length (in.)	Weight (lb)	MC (%)	Specific gravity	MOE ($\times 10^6$ lb/in^2)	Time to failure (min:s)	Failure load (lb)	MOR (lb/in^2)	Comment
363	3.41	1.47	68.63	6.7	21.7	0.44	1.51	6.1	2,400	7,344	Splintering tension near knot
376	3.45	1.45	68.63	6.3	23.5	0.37	0.92	3.15	1,310	3,996	Tension failure near knot
377	3.44	1.44	68.63	6.7	26.9	0.45	1.41	6.37	2,175	6,695	Brash tensile failure
381	3.44	1.45	68.63	6.4	24.6	0.38	1.48	5.25	2,260	6,899	Splintering tension near knot
386	3.45	1.44	68.63	6.8	22.3	0.42	1.60	5.16	2,275	6,991	Slope of grain
387	3.88	1.88	68.63	6.4	24.2	0.41	0.47	3.31	1,095	2,042	Tensile separation from knot
388	3.44	1.46	68.63	5.7	25.6	0.36	1.49	4.35	2,120	6,432	Splintering tension
395	3.41	1.45	68.63	7.6	26.1	0.50	1.46	3.52	2,100	6,577	Tensile separation
396	3.44	1.47	68.63	5.7	23.9	0.36	1.03	4.4	1,710	5,163	Splintering tension near knot
398	3.50	1.44	68.63	7.0	42.9	0.37	1.34	5.25	1,870	5,575	Tension failure near knot
399	3.47	1.44	68.63	6.0	30.3	0.37	1.28	4.47	1,880	5,706	Splintering tension
402	3.31	1.44	68.63	6.4	32.8	0.38	1.37	7.59	1,990	6,624	Tension failure near spike knot
404	3.46	1.46	68.63	9.1	29.7	0.38	2.11	7.21	3,105	9,319	Brash failure
405	3.46	1.45	68.63	6.5	30.7	0.55	0.93	3.42	1,172	3,534	Tension failure near knot
408	3.43	1.48	68.63	6.7	24.6	0.45	1.45	7.06	2,190	6,588	Splintering tension
410	3.43	1.45	68.63	5.5	20.5	0.47	1.31	3.49	1,650	5,103	Splintering tension
411	3.41	1.41	68.63	6.4	25.3	0.40	1.47	5.03	1,710	5,502	Tension failure
413	3.47	1.38	68.63	7.8	24.8	0.50	1.49	8.18	2,110	6,696	Splintering tension near knot
415	3.38	1.44	68.63	4.5	12.6	0.33	1.17	3.53	1,840	5,900	Splintering tension failure
417	3.44	1.46	68.63	8.6	29.1	0.55	1.33	5.36	2,110	6,421	Tension separation around knot
423	3.45	1.43	68.63	6.7	46.2	0.35	1.04	6.03	1,770	5,465	Tension/slope-of-grain failure
424	3.45	1.45	68.63	7.4	33.4	0.42	1.39	5.57	2,240	6,844	Splintering tension
429	3.44	1.49	68.63	7.1	24.3	0.44	1.71	7.37	2,610	7,769	Splintering tension
433	3.45	1.44	68.63	7.6	23.2	0.47	1.60	6.53	2,460	7,499	Tension failure near knot
435	3.46	1.46	68.63	6.0	25.6	0.36	1.18	5.14	1,950	5,862	Tension failure
438	3.44	1.44	68.63	7.7	61.6	0.37	1.35	4.09	1,680	5,150	Tension failure
443	3.46	1.46	68.63	6.7	33.4	0.41	1.30	6.02	2,020	6,062	Splintering tension
447	3.48	1.43	68.63	6.8	26.3	0.42	1.29	6.08	2,135	6,473	Splintering tension near knot
450	3.44	1.44	68.63	6.5	19.6	0.44	1.53	4.44	2,810	8,628	Splintering tension
451	3.49	1.46	68.63	7.1	24.4	0.44	1.36	5.25	2,250	6,637	Splintering tension
453	3.43	1.46	68.63	6.3	24.4	0.40	1.14	7.17	1,910	5,825	Splintering tension from knot
456	3.44	1.52	68.63	8.5	26.2	0.40	1.09	5.18	1,160	3,397	Splintering tension from knot
467	3.45	1.44	68.63	6.7	22.1	0.43	1.62	7.15	2,750	8,430	Tension/slope of grain failure
468	3.44	1.45	68.63	7.6	23.8	0.48	1.74	6.42	2,400	7,326	Splintering tension
470	3.43	1.47	68.63	5.5	25.8	0.39	1.16	7.07	2,110	6,423	Splintering tension
471	3.38	1.43	68.63	7.2	20.5	0.48	1.75	4.26	1,540	4,943	Tension failure at knot
472	3.44	1.45	68.63	7.3	20.9	0.48	1.94	4.33	2,905	8,908	Slope of grain
473	3.45	1.46	68.63	5.5	27.6	0.40	1.27	6.12	1,560	4,734	Tension failure at knot
474	3.42	1.44	68.63	7.3	20.5	0.40	1.32	5.58	2,270	7,101	Splintering tension
475	3.44	1.43	68.63	5.9	20.7	0.38	1.06	3.48	1,500	4,669	Tension failure at knot